Molecular Therapy
Original Article

Epidermal E-Cadherin Dependent β-Catenin Pathway Is Phytochemical Inducible and Accelerates Anagen Hair Cycling

Noha S. Ahmed,[1,2,5] Subhadip Ghatak,[1,5] Mohamed S. El Masry,[1,3,5] Surya C. Gnyawali,[1] Sashwati Roy,[1] Mohamed Amer,[2] Helen Everts,[4] Chandan K. Sen,[1] and Savita Khanna[1]

[1]Department of Surgery, Davis Heart and Lung Research Institute, Center for Regenerative Medicine & Cell-Based Therapies, Wexner Medical Center, The Ohio State University, Columbus, OH 43210, USA; [2]Department of Dermatology and Venereology, Zagazig University, 44519 Zagazig, Egypt; [3]Department of General Surgery (Plastic Surgery Unit), Zagazig University, 44519 Zagazig, Egypt; [4]Department of Nutrition and Food Sciences, Texas Woman's University, Denton, TX 76204, USA

Unlike the epidermis, which regenerates continually, hair follicles anchored in the subcutis periodically regenerate by spontaneous repetitive cycles of growth (anagen), degeneration (catagen), and rest (telogen). The loss of hair follicles in response to injuries or pathologies such as alopecia endangers certain inherent functions of the skin. Thus, it is of interest to understand mechanisms underlying follicular regeneration in adults. In this work, a phytochemical rich in the natural vitamin E tocotrienol (TRF) served as a productive tool to unveil a novel epidermal pathway of hair follicular regeneration. Topical TRF application markedly induced epidermal hair follicle development akin to that during fetal skin development. This was observed in the skin of healthy as well as diabetic mice, which are known to be resistant to anagen hair cycling. TRF suppressed epidermal E-cadherin followed by 4-fold induction of β-catenin and its nuclear translocation. Nuclear β-catenin interacted with Tcf3. Such sequestration of Tcf3 from its otherwise known function to repress pluripotent factors induced the plasticity factors Oct4, Sox9, Klf4, c-Myc, and Nanog. Pharmacological inhibition of β-catenin arrested anagen hair cycling by TRF. This work reports epidermal E-cadherin/β-catenin as a novel pathway capable of inducing developmental folliculogenesis in the adult skin.

INTRODUCTION

Mammalian hair follicles harbor a multipotent stem cell niche of diverse developmental origin that continuously self-renew, differentiate, regulate hair growth, and contribute to skin homeostasis. Hair follicle neogenesis may also replenish the stem cell pool for skin rejuvenation and regenerative healing.[1] Post-natal hair follicles regenerate periodically by spontaneous cycle of growth (anagen), apoptosis-driven regression (catagen), and relative quiescence (telogen).[2] Developmentally, hair follicle morphogenesis takes place during the late embryonic and early neonatal periods.[3,4] It begins with the formation of a small cluster of epithelial placodes that is marked by the expression of cytokeratin 17 and Lgr6.[5,6] However, de novo formation of hair follicles is typically not observed in adults, except during wound-induced activation of the epidermal Wnt/β-catenin pathway.[7–9]

Our previous works recognized tocotrienol as a potent neuroprotective agent.[10–14] Compared to the widely known form of vitamin E tocopherol, tocotrienol has a similar phenolic head. However, instead of saturated phytyl tail in tocopherol, tocotrienol has an isoprenoid tail.[15] During studies testing the effect of tocotrienol on peripheral neuropathy, we were struck by an unexpected observation that murine skin topically treated with tocotrienol showed more robust hair growth. Although there is anecdotal evidence reported in the literature claiming improvement of hair growth in humans by tocotrienol,[16] the underlying mechanisms remain elusive. Thus, the objective of the present study was to unveil the mechanism of tocotrienol-induced hair folliculogenesis in the adult skin.

RESULTS

Induction of Anagen Hair Cycling in Skin

Topical application of tocotrienol-rich fraction (TRF) on depilated murine dorsal skin induced anagen hair growth, as detected by skin color change from pink to black (Figure 1A). Higher magnification images using Dermascope (Cyberderm) showed thick, black hair shafts of anagen hairs in the TRF-treated group, compared to the telogen hairs of the corresponding placebo (PBO) group at day 21 (Figure 1B). H&E staining revealed a significant increase in the number of anagen hair follicles extending deep into subcutaneous fat following TRF treatment (Figures 1C and S1A). Enumeration of hair follicles showed significant increase in the number of anagen hair follicles at days 7, 14, and 21 following TRF treatment (Figure 1C). Anagen transition in leptin-receptor-deficient db/db mice is known to be retarded,

Received 25 January 2017; accepted 16 July 2017;
http://dx.doi.org/10.1016/j.ymthe.2017.07.010.

[5]These authors contributed equally to this work.

Correspondence: Savita Khanna, PhD, Associate Professor of Surgery, The Ohio State University Wexner Medical Center, 473 West 12th Avenue, Columbus, OH 43210, USA.
E-mail: savita.khanna@osumc.edu

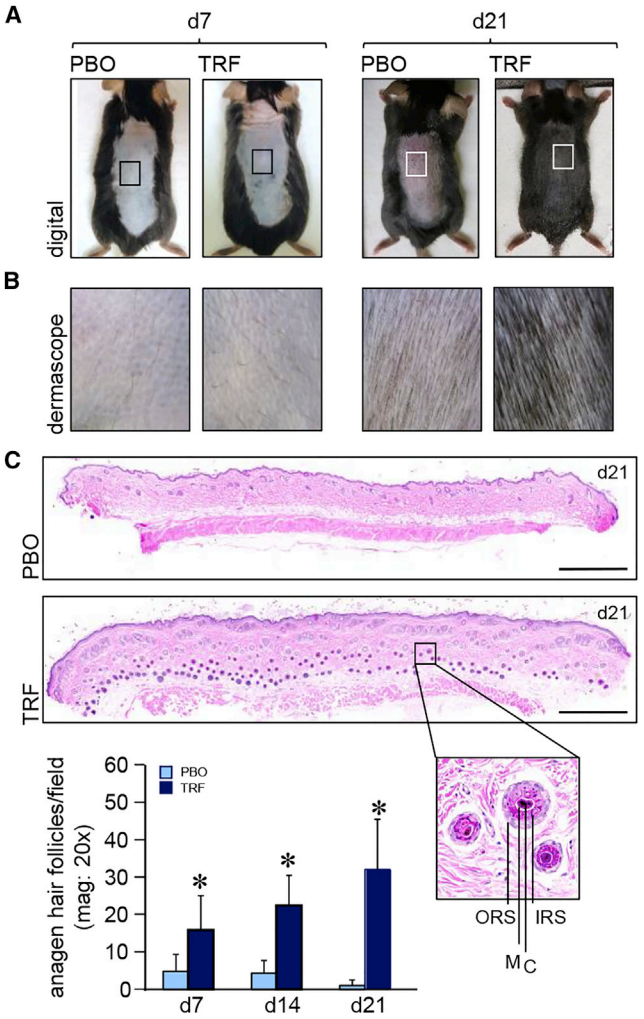

Figure 1. Induction of Epidermal Anagen Hair Cycling in Skin

(A) Photomicrographs of mouse dorsal skin at day 7 and day 21 showing induction of anagen hair cycling in TRF-treated shaved skin. (B) Dermascopic images from insets in (A) of the dorsal mouse skin at day 7 and day 21. TRF induced anagen hair on day 21. (C) Photomicrograph of formalin-fixed, paraffin-embedded H&E-stained sections showing more anagen hair follicles with dermal papillae reaching the subcutaneous fat layer in TRF-treated sections at day 21. Scale bars, 500 μm. Inset: close-up of a hair follicle with outer root sheath (ORS), inner root sheath (IRS), cortex (C), and medulla (M). Hair follicles were quantified from H&E-stained sections. Data are mean ± SD (n = 6). *p < 0.001.

compared to wild-type (WT) mice[17] (Figure S1B). To study the effect of TRF on anagen hair cycling in db/db mice, TRF was applied on depilated dorsal skin of db/db mice for 21 days. While the PBO mouse group remained in telogen phase, as noted by the pink color of the dorsal skin, TRF-treated mice showed induction of anagen, as evident by the black color of dorsal skin at day 21 (Figure S1C). Histomorphometric quantitation of the number of anagen hair follicles in db/db mice showed a significant increase in the TRF group, compared with the corresponding PBO group, where the hair follicles remained in telogen phase (Figure S1D).

Developmental Hair Folliculogenesis in the Adult Skin

LGR6, a fetal stem cell marker, is abundant in fetal murine skin (Figure 2A). TRF induced LGR6 in the adult skin (Figure 2A). Characteristic features of hair follicle development, such as "placode," "hair germ," "hair peg" and "bulbous peg," were evident in murine fetal skin (embryos on day 18.5 of gestation [E18.5]) (Figure 2B). Such characteristics were not shared by the adult skin. However, topical TRF application for 7 days resulted in the manifestation of the above mentioned fetal characteristics of hair follicular development in the adult skin (Figure 2C).

Epidermal Keratinocyte Proliferation

While sharply minimized in homeostatic adult skin, active cell proliferation is a hallmark characteristic of developing fetal skin.[18] Topical application of TRF stimulated skin cell proliferation, as detected in *rep*TOP*mito*IRE mice using an in vivo imaging system (IVIS) (Figure 3A). This observation was substantiated by immunohistochemical studies demonstrating the presence of $Ki67^{+}$ cells in the epidermis and hair follicles (Figure 3B). Such keratinocyte proliferation caused by topical TRF application resulted in epidermal thickening (Figure 3C).

Epidermal Junctional Protein Expression in Hair Folliculogenesis

Of the five junctional proteins studied—i.e., claudin, occludins, ZO-1, ZO-2, and E-cadherin—topical TRF treatment significantly decreased the expression of claudin, ZO-2, and E-cadherin expression (Figure 4A). No such change was observed in ZO-1 and occludin (Figure S2A). Consistent with its effect on suppressing the above mentioned three junctional proteins, topical TRF treatment partly compromised skin barrier function (Figure 4B). In vitro studies with human keratinocytes (HaCaT cells) showed that exposure to pure tocotrienol causes a sharp decrease in membrane E-cadherin expression associated with nuclear translocation of β-catenin (Figure 4C). Such nuclear translocation of β-catenin was also observed when HaCaT cells were exposed to TRF (Figure S2B).

Inducible β-Catenin Expression and Nuclear Translocation

In developmental folliculogenesis, β-catenin represents a major signaling hub.[19] In keratinocytes of developing fetal skin, activated β-catenin is primarily localized in the nucleus (Figure S3A). Topical application of TRF on adult murine skin resulted in potent induction and activation of epidermal β-catenin, as manifested by higher expression and nuclear translocation (Figures 5A, 5B, and S3B). Such observation, akin to the fetal phenotype, is in contrast with what is typically observed in the resting adult skin (Figure S3B). In human keratinocytes, knockdown of E-cadherin caused the translocation of membrane and cytosolic β-catenin to the nucleus (Figure S3C). In the nucleus, β-catenin directly interacted with the transcription factor 3 (Tcf3) (Figures 5C and S3D–S3F). Tcf3 is known to repress pluripotency factors.[20] Functional significance of observed β-catenin-Tcf3 binding and sequestration of Tcf3 following TRF treatment was defined by the observation demonstrating elevated levels of skin-specific pluripotency factors KLF4, c-MYC,

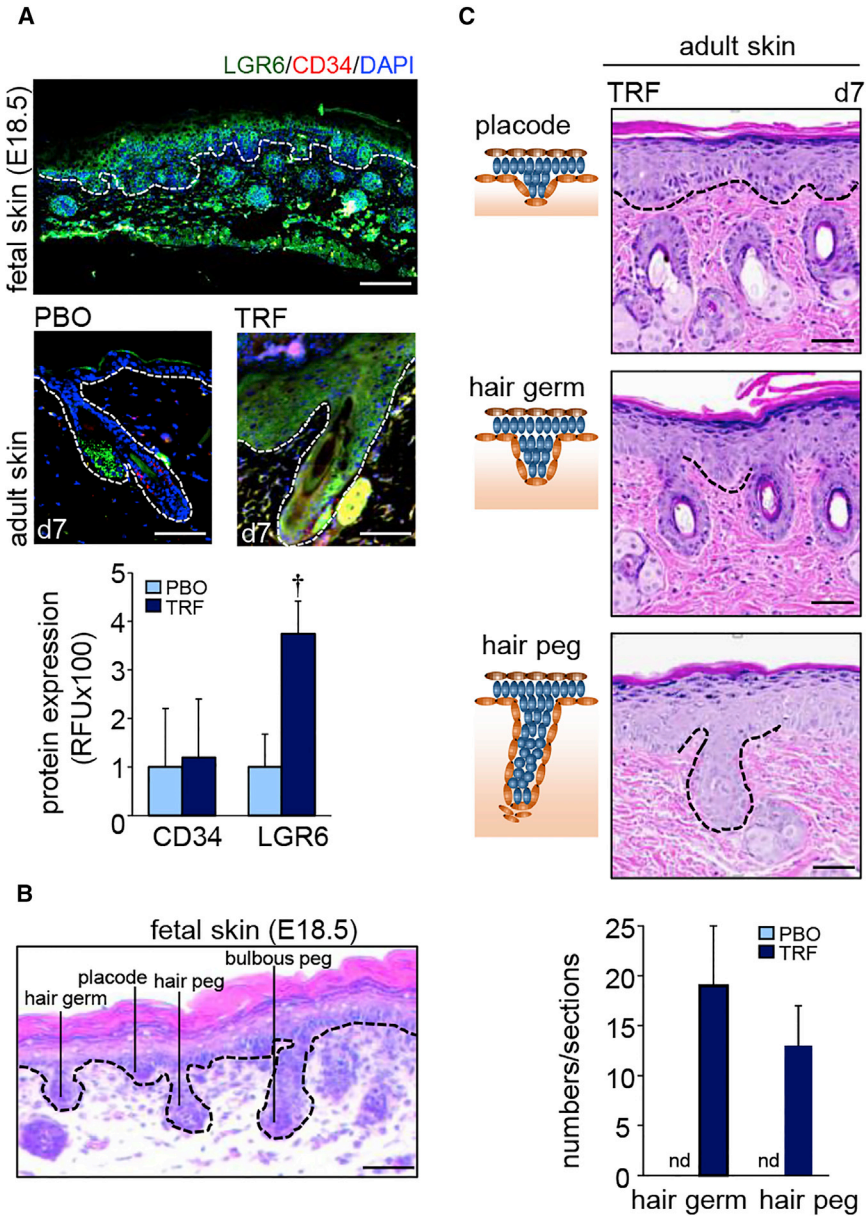

Figure 2. Developmental Hair Folliculogenesis

(A) LGR6 and CD34 immunostaining counterstained with nuclear DAPI. Upper panel: LGR6 (green) and CD34 (red) in fetal skin. Scale bar, 100 μm. Bottom panel: Adult skin. Scale bars, 50 μm. Epidermal and dermal junction is marked by white dashed lines. Fluorescence is plotted as relative florescence units (RFUs). Data are mean ± SD (n = 3). †p < 0.01. (B) H&E-stained section showing development of hair follicle from the fetal skin epidermis. Scale bar, 50 μm. (C) TRF treatment on adult skin showed morphological characteristics similar to those of murine fetal skin. Schematic diagrams are shown in the left-hand panels, while actual regions are marked with dashed lines in the H&E-stained sections in the right-hand panels. Scale bars, 50 μm. The number of "hair germ" and "hair peg" features were quantified from H&E-stained sections and expressed graphically (n = 6). nd, not detected.

and NANOG[21] in epidermal cells (Figure S3G). Gene expression data from laser-captured epidermis (Figure S3H) revealed that TRF-induced binding of β-catenin with Tcf3 resulted in the upregulation of *sox9*, *oct4*, and *lgr6* (Figure S3I). Furthermore, immunohistochemical analyses showed robust expression of SOX9, OCT4, K17, and K15 in the TRF-treated adult murine epidermis (Figures 5D and S3J).

Significance of β-Catenin-Tcf3 Interaction in the Induction of Pluripotency

A fluorescein amidite (FAM)-labeled oligodeoxynucleotide construct, based on Tcf3 binding consensus sequence as described previously,[22,23] was used as a decoy to circumvent transactivation caused by the β-catenin-Tcf3 complex. Negative-control oligodeoxynucleotides with eight-base mismatch served as scrambled control (Figure 6A). This strategy was based on the competition of β-catenin-bound Tcf3, under conditions of tocotrienol treatment, to bind to endogenous target sequence in the presence of exogenous abundant Tcf3 decoy (Figure 6B). In the presence of the aforementioned decoy double-stranded oligonucleotide, the induction of stemness, as well as pluripotency factors in response to tocotrienol treatment, was markedly blunted. Quantitative immunocytochemistry (ICC) results for SOX9, OCT4, K17, and K15 are shown in Figure 6C. Additionally, findings on the expression of KLF4, c-MYC, and NANOG in human keratinocytes are presented as supplemental data (Figures S4A and S4B).

Pharmacological Inhibition of Inducible Anagen Hair Cycling

The significance of β-catenin in TRF-induced anagen hair cycling in adult murine skin was tested using IWR-1, a pharmacological inhibitor of β-catenin (Figure S4C). Topical pre-treatment of the murine adult skin with IWR-1 (Figure S5A) significantly decreased the number of anagen hair follicles induced by topical TRF application (Figure S5B). Such observation was associated with the finding that IWR-1 is also capable of eliminating the effect of TRF on stimulating keratinocyte proliferation (Figure S5C). Topical IWR-1 pre-treatment was effective in degrading epidermal β-catenin (Figure 7A). Interestingly, IWR-1 pre-treatment did not influence the lowering of E-cadherin in response to TRF (Figure 7B). Thus, the ability of topical TRF treatment to induce epidermal proliferation and hair folliculogenesis in the adult skin was significantly impaired by IWR-1 (Figures S5B and S5C). This observation suggests that, in the pathway of TRF-induced folliculogenesis, E-cadherin resides upstream of β-catenin (Figure 7C).

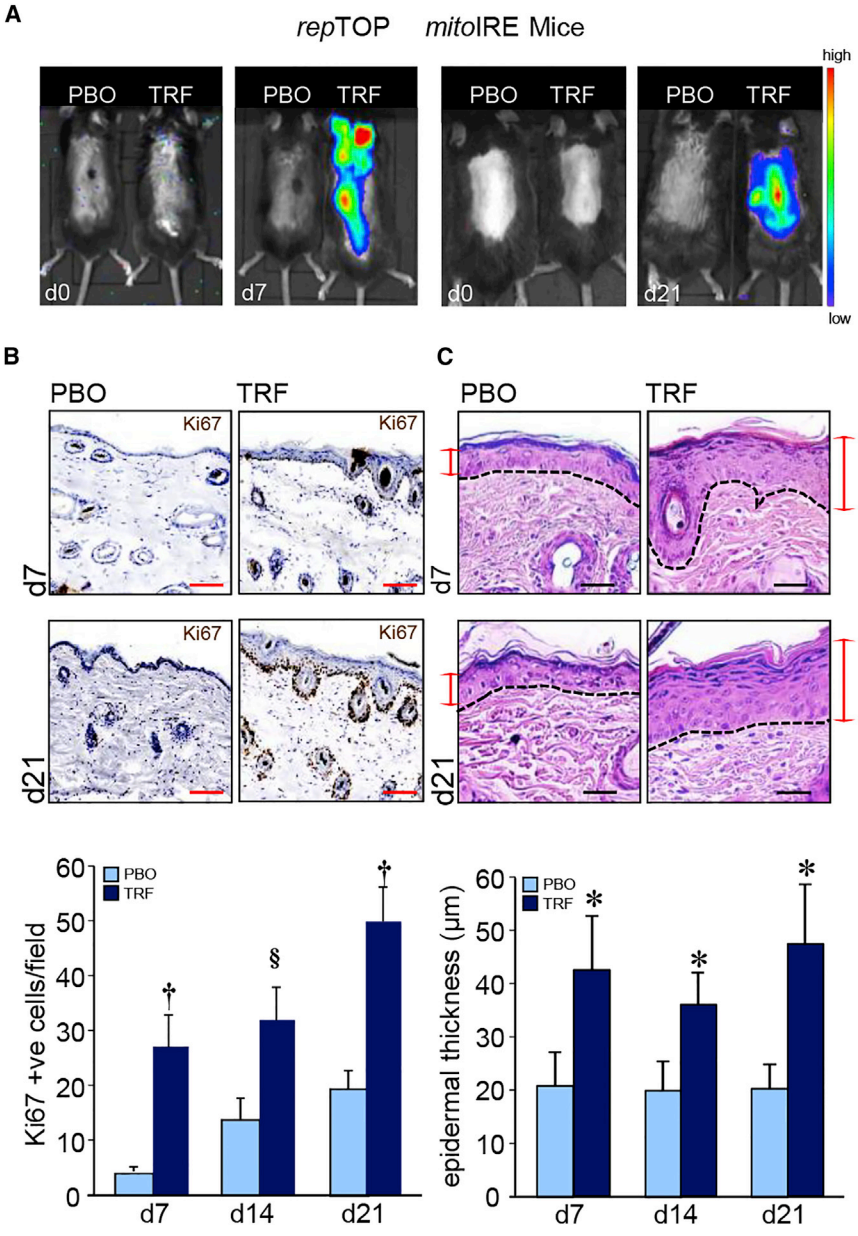

Figure 3. Keratinocyte Proliferation in Hair Folliculogenesis

(A) IVIS image from *rep*TOP*mito*IRE showing cell proliferation in animals treated with TRF or placebo (PBO) on days 7 and 21. (B) Immunohistochemical localization of Ki67 in paraffin sections of mouse skin showing the abundance of $Ki67^+$ cells in mice treated (days 7 and 21) with TRF compared to PBO. Scale bars, 50 μm. $Ki67^+$ cells were quantified and plotted graphically. Data are mean ± SD (n = 3) $^{\S}p < 0.05$; $^{\dagger}p < 0.01$. (C) Photomicrograph of H&E-stained paraffin sections showing epidermal thickening in mice treated (days 7 and 21) with TRF. The dermal and epidermal junctions are each marked by a dashed line. Scale bars, 20 μm. Epidermal thickness was quantified and plotted graphically. Data are mean ± SD (n = 4). $^{*}p < 0.001$.

DISCUSSION

Hair follicles serve multiple critical functions.[2,24] They undergo cyclic transformations between phases of rapid growth (anagen), apoptosis-driven regression (catagen), and relative quiescence (telogen). With every cycle, the hair follicle regenerates itself. The result is daughter-cell populations, which are derived from resident epithelial, neural, and mesenchymal stem cells.[25,26] In adults, during each cycle, a new hair shaft is formed, and the old hair is eventually shed mostly by an actively regulated exogen.[2] In the adult skin, generation of the new hair shaft depends on the activation of hair-specific epithelial stem cells that are harbored in the bulge region of the hair follicle epithelium. Development of hair follicles during fetal skin morphogenesis is preceded by active epidermal cell proliferation.[27] Although the processes of adult hair follicle and fetal hair follicle formation have several contrasting features, it is evident that the adult skin may acquire plasticity by activation of key signaling molecules such as β-catenin.[28]

β-Catenin has emerged as a key signaling hub for hair follicle formation in both adult and fetal states. Transient β-catenin activation advances telogen to anagen.[29] Within epidermal keratinocytes, β-catenin is localized in three major compartments: the plasma membrane, the cytoplasm, and the nucleus.[30] The β-catenin signaling pathway is evolutionarily conserved.[31] Nuclear translocation followed by subsequent binding to repressor transcription factor Tcf3 assigns the function of transcriptional activators to β-catenin.[32,33] Epithelial integrity during adult skin homeostasis is achieved by the binding of β-catenin with E-cadherin in the plasma membrane.[34] Such membrane binding with the intracellular domain of E-cadherin[30] restrains the function of β-catenin as transcriptional activator. Thus, E-cadherin plays a critical role in the stabilization and in determining the function of β-catenin.[34] This work reports the first evidence demonstrating that conditions resulting in the loss of membrane E-cadherin may release and activate β-catenin. Interestingly, such form of β-catenin activation was achieved by the topical application of a phytochemical. Pure tocotrienol, the seed form of natural vitamin E, which is a major component of TRF,[10,15] markedly depleted membrane E-cadherin, releasing β-catenin for nuclear translocation. Under such conditions, nuclear β-catenin binds to Tcf3, blocking its repressive action on cell plasticity factors.[35] As a result, cell stemness and pluripotency were induced. Such effect of tocotrienol was blunted in the presence of a decoy oligonucleotide

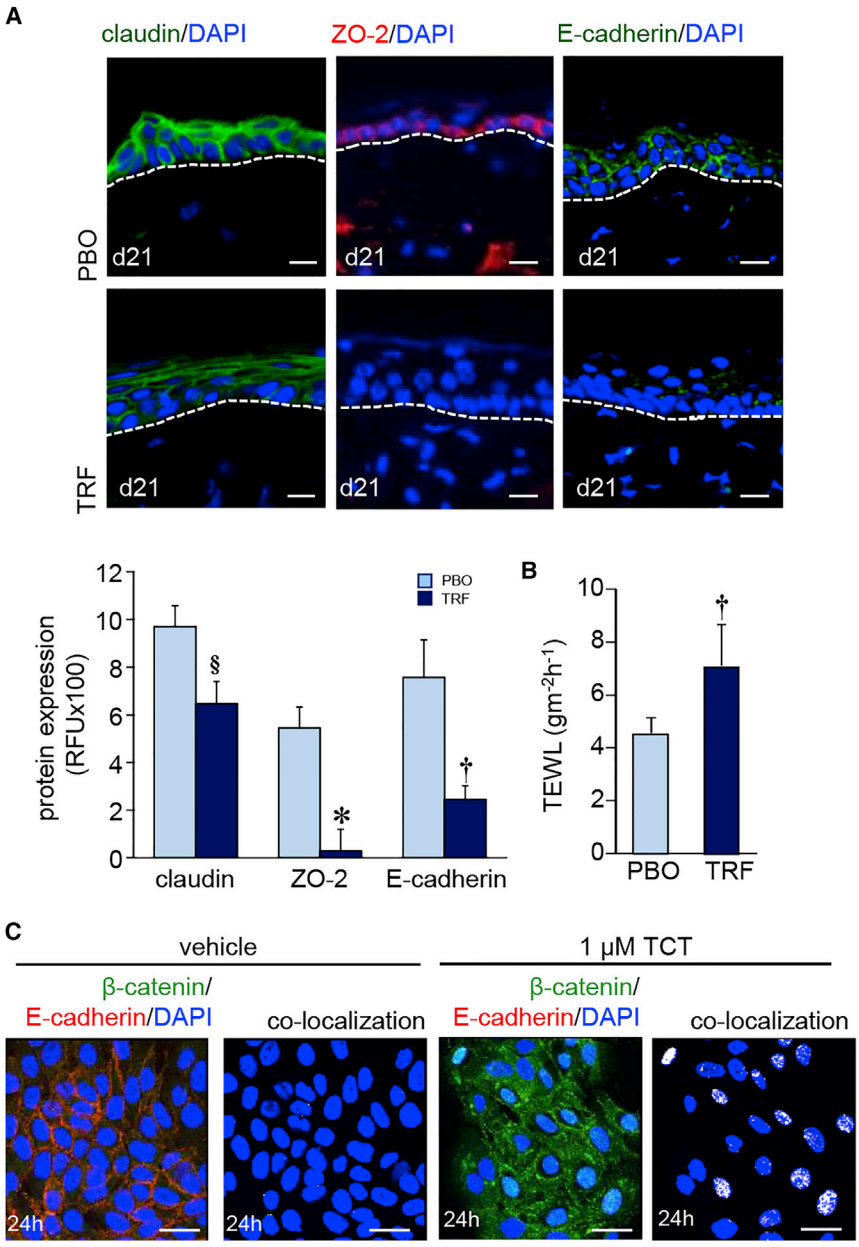

Figure 4. Epidermal Junctional Proteins in Murine Skin Folliculogenesis

(A) TRF lowered (day 21) the expression of claudin (green), ZO-2 (red), and E-cadherin (green) in murine skin. Sections were counterstained with DAPI. Dermal-epidermal junction is indicated by dashed white line. Scale bars, 20 μm. Abundance of junctional proteins in (A) were quantified and expressed graphically as mean ± SD (n = 6). $^{§}p < 0.05$; $^{†}p < 0.01$; $^{*}p < 0.001$. (B) Trans-epidermal water loss (TEWL) was measured from the dorsal skin of mice after topical application of TRF or PBO for 21 days. Data are mean ± SD (n = 6). $^{†}p < 0.01$. (C) Keratinocytes (HaCaT cells) treated with pure tocotrienol (1 μM, 24 hr) showed lower expression of E-cadherin (red) in the cell membrane and increased nuclear translocation of β-catenin (green). Scale bars, 20 μm.

designed to limit the binding of Tcf3 to its endogenous consensus sites, establishing the withdrawal of Tcf3 as transcription factor as a central mechanism responsible for tocotrienol action.

In vivo studies showed that TRF application decreased junctional protein E-cadherin in the skin. Released from the membrane, β-catenin becomes available for nuclear translocation. This process can be intercepted by the degradation of cytosolic β-catenin by the pharmacological inhibitor IWR-1.[36] Thus, TRF-induced mobilization of β-catenin did not influence the Tcf3 function in the presence of IWR-1. This observation demonstrates that the effect of TRF on hair follicle formation is dependent on loss of E-cadherin and activation of β-catenin. The study of TRF function helped to elucidate a novel β-catenin pathway that relies on the loss of upstream E-cadherin for its activation. Epithelial placodes, characteristic of the murine embryonic hair follicle development, invaginate to give rise to the germ by E15.5, the peg by E17.5, and the bulbous peg by E18.5.[3] This work reports the first evidence of placode, hair peg, and hair germ during the course of adult hair folliculogenesis. Once the bud proliferates, it encases the dermal papilla and further differentiates to form the hair shaft.[37]

Diabetic complications include impaired induction of anagen.[17,38] Leptin, an adiponectin, also acts as anagen inducer.[39] Leptin receptor is highly expressed in dermal cells, including the dermal papilla that is critical for hair follicle morphogenesis.[38] During hair follicle development, dermal papillae are formed by epithelial condensate to form mature dermal papillae.[40] This work shows that it is possible to induce anagen under diabetic conditions. This observation supports the contention that TRF, the inducer of anagen in the diabetic skin, acts upstream of dermal papilla formation to induce anagen. Given that dermal papilla formation is necessary for the induction of anagen in the adult skin, our observation leads to the notion that TRF induces anagen in the diabetic skin via a pathway akin to that during fetal skin development. Such pathway involves the activation of β-catenin and the formation of placode.[3,41]

The post-natal skin does not generate any new hair follicles.[42] Thus, growth of hair follicles in the adult skin relies on the hair follicular regeneration process contributed by the stem cell niche of existing

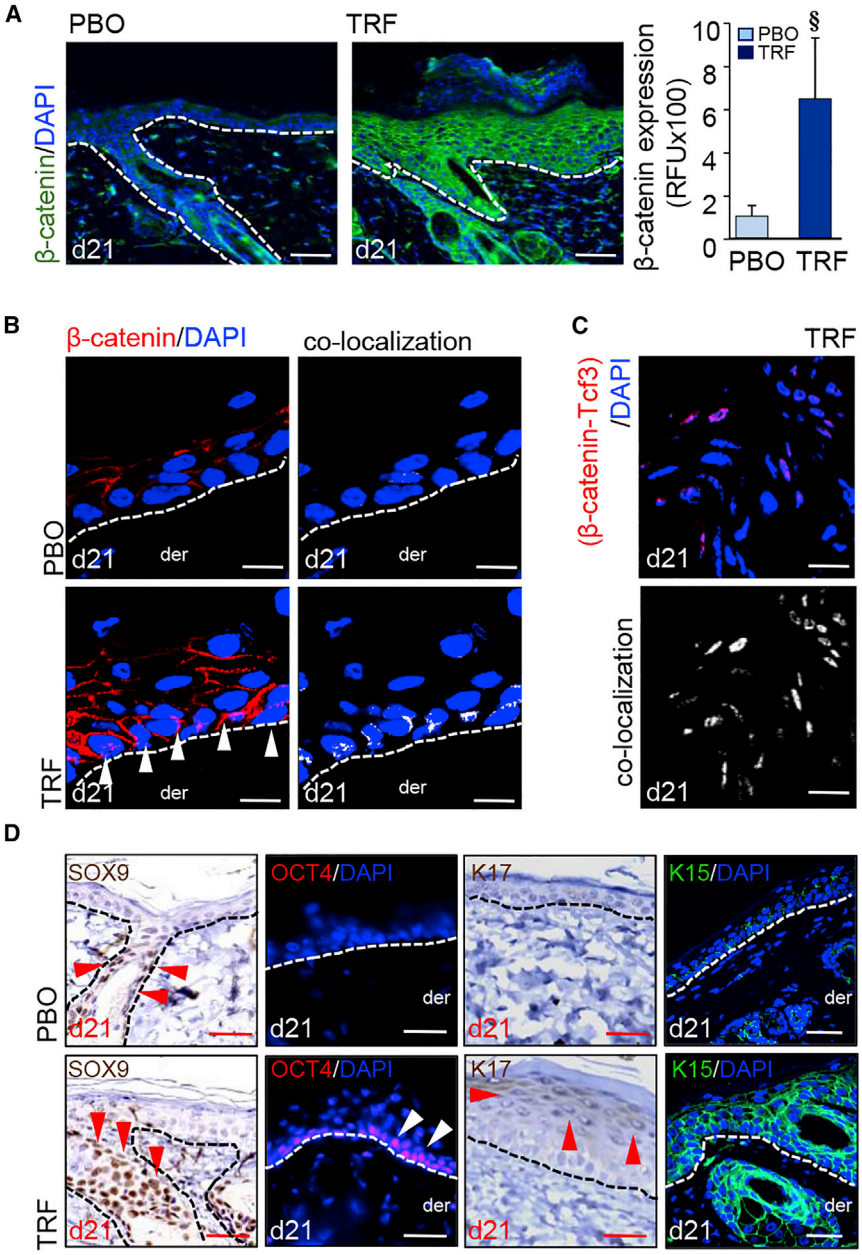

Figure 5. Induction of β-Catenin and Nuclear Translocation

(A) TRF-induced (day 21) β-catenin (green) in murine epidermis. Counterstained with DAPI (blue). Scale bars, 50 μm. Fluorescence intensity was plotted graphically. Data are mean ± SD (n = 3). $^{§}p < 0.05$. (B) Confocal microscopy showing TRF-induced translocation (day 21) of β-catenin into the nucleus. Counterstained with DAPI. Dermal (der) and epidermal junction indicated by a white dashed line. Scale bars, 10 μm. (C) Proximity ligation assay (PLA) showed β-catenin-Tcf3 co-localization in the nucleus in TRF treated adult skin. Scale bars, 10 μm. (D) Robust expression of SOX9, OCT4, K15, and K17 in TRF-treated (day 21) adult skin epidermis. The arrowhead indicates positive signals: red for DAB staining and white for fluorescent staining. Scale bars, 20 μm.

follicles.[43] To serve this purpose, and for the maintenance of epidermis, reservoirs of multipotent epithelial stem cells are set aside at the base of the hair follicle "bulge."[44,45] Follicle stem cells are activated at the telogen-to-anagen transition to initiate a new round of hair growth. Hair follicular stem cells undergo multiple sessions of activity, during which hair and skin regeneration occurs.[46] Hair follicles are a major contributor to the overall stem cell pool of the adult skin.[43] Thus, follicular growth in the adult skin may markedly enhance stem cell abundance in this largest organ of the body. A rapidly growing body of evidence directly implicates follicular stem cells in skin functions such as turnover and maintenance of the adult skin, management of age-related complications, improved tissue repair, and protection against UV damage. It is, therefore, plausible that substantial induction of hair follicles in the adult skin by TRF will influence skin function and fate as it relates to the aforementioned conditions and complications, as well as their derivatives such as sunburn, melanoma, and psoriasis.

Both murine and human hair follicles have comparable cell types that undergo repetitive cycles of active growth (anagen), regression (catagen), and quiescence (telogen).[2,47–49] However, one of the major differences between human and murine hair follicles is that, in the mouse skin, the anagen phase lasts for only 2–3 weeks, whereas in humans, it lasts for several years.[50–52] Consistent with the finding of our work, Beoy et al. reported induction of hair growth by TRF in humans.[16] TRF represents a rich, natural source of tocotrienol that is readily accessible and generally recognized as safe by the Food and Drug Administration (FDA; GRN no. 307). It is, thus, well suited for human intervention. Therefore, all in vivo studies in this work were conducted using TRF. An emphasis on elucidating the mechanistic underpinnings of how TRF-induced anagen hair cycling necessitated the study of pure α-tocotrienol, a major component of TRF, in all in vitro experiments.

In summary, this work presents first evidence, on a number of fronts, demonstrating that it is possible to induce anagen hair follicle development in the adult skin via a pathway akin to that during fetal skin development. Such a pathway, inducible by topical phytochemical treatment, is capable of inducing follicular growth in the adult diabetic skin, which is otherwise known to be refractory to the induction of anagen. Downregulation of epithelial E-cadherin is recognized as a

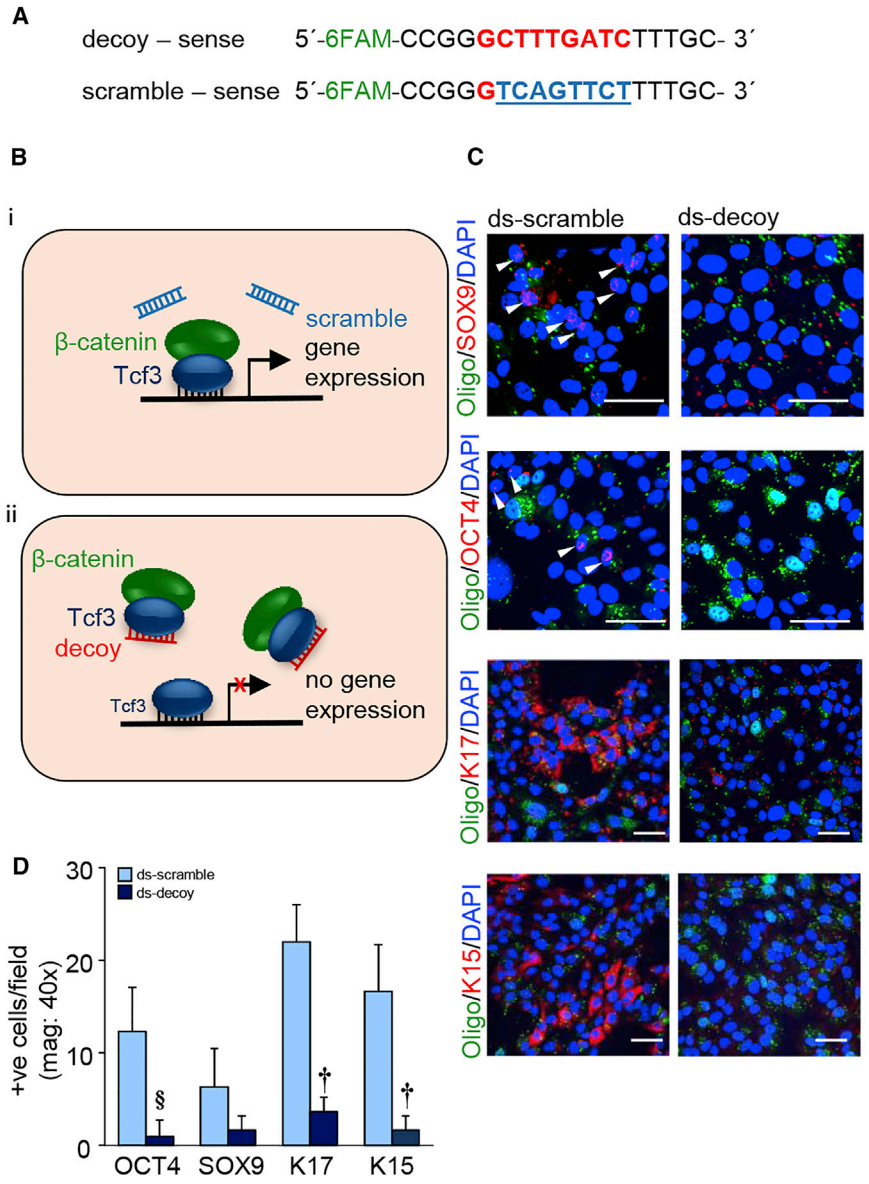

Figure 6. β-Catenin-Tcf3 Interaction in Induction of Pluripotency

(A) Design of FAM-labeled TCF decoy and eight-base mismatch scramble control. (B) Theoretical scheme of Tcf3 decoy strategy. (i) Normal β-catenin signaling. β-catenin/Tcf3 complex binding facilitates gene expression. (ii) β-catenin may preferentially bind to the Tcf3 decoy region, which competitively inhibits target gene activation. (C) Expression of SOX9, OCT4, K17, and K15 in Tcf3 scramble (0.1 μM) and decoy (0.1 μM) transfected cells after pure tocotrienol treatment (1 μM, 24 hr). The arrowhead indicates positive signals. Scale bars, 50 μm. (D) The number of positive cells per field was quantified and plotted graphically. Data are mean ± SD (n = 3). $^{§}p < 0.05$; $^{†}p < 0.01$.

trigger for β-catenin activation, which sequesters Tcf3, unleashing hair follicular regeneration. Beyond its role in the growth of hair, hair follicles serve as stem cell reservoirs that may influence numerous aspects of skin function and complication. Thus, novel strategies to induce follicular proliferation in the adult skin are likely to have a wide range of implications in preserving and restoring skin function.

MATERIALS AND METHODS

Animal and Experimental Design

Male C57BL/6 mice were obtained from Harlan Laboratory. Male mice homozygous (BKS.Cg-$m^{+/+}$ $Lepr^{db/J}$ or db/db; stock no 000642) for spontaneous mutation of the leptin receptor ($Lepr^{db}$) were obtained from Jackson Laboratory. Male *rep*TOP *mito*IRE mice were obtained from Charles River Laboratories. These mice have a luciferase reporter tagged with the cyclin B2 promoter. Thus, administration of luciferin at a dose of 100 mg/kg body weight i.p. (intraperitoneally) produces bioluminescence from any proliferating cell of the body.[53] All animals were 7–8 weeks old at the start of the experiment. All animal studies were performed in accordance with protocols approved by the Laboratory Animal Care and Use Committee of The Ohio State University.

TRF was obtained from commercially available Tocovid SupraBio capsules.[54] Each capsule contains Tocomin 50%, which typically provides 61.52 mg d-alpha-tocotrienol, 112.80 mg d-gamma-tocotrienol, 25.68 mg d-delta-tocotrienol, 91.60 IU d-alpha-tocopherol, 51.28 mg plant squalene, 20.48 mg phytosterol complex, and 360.00 μg phytocarotenoid complex. Thus, each capsule contains 144.86 mM of d-alpha-tocotrienol. In the placebo, the tocotrienol was replaced by soya oil. For in vitro experiments, pure tocotrienol was provided by Excelvite.

Mice were randomly (http://www.random.org) divided into different groups, as indicated in the corresponding figure legends. The dorsal skin was shaved, and hair was depilated using Nair 2 days before experiments. TRF, or its PBO, was applied topically at a dose of 5 mg/cm^2 skin, thrice per week. During the procedure, mice were anesthetized by low-dose isoflurane inhalation. Digital photographs were collected (Canon PowerShot S6 and Dermascope from Dino-Lite Pro II). In some experiments, to inhibit β-catenin expression, IWR-1 (Sigma; I0161) was used. A 10% DMSO stock IWR-1 solution was prepared and diluted with glycerol to a final concentration of 2 μg/0.5 cm^2 skin. This solution was applied topically on the dorsal skin of C57BL/6 mice at a dose of 12.5 μL/0.5 cm^2 skin for 4 consecutive days of IWR-1 or vehicle, followed by 7 consecutive days of IWR-1 or vehicle for 1 hr under occlusive dressing (Tegaderm, 3M). Such inhibitor treatment was

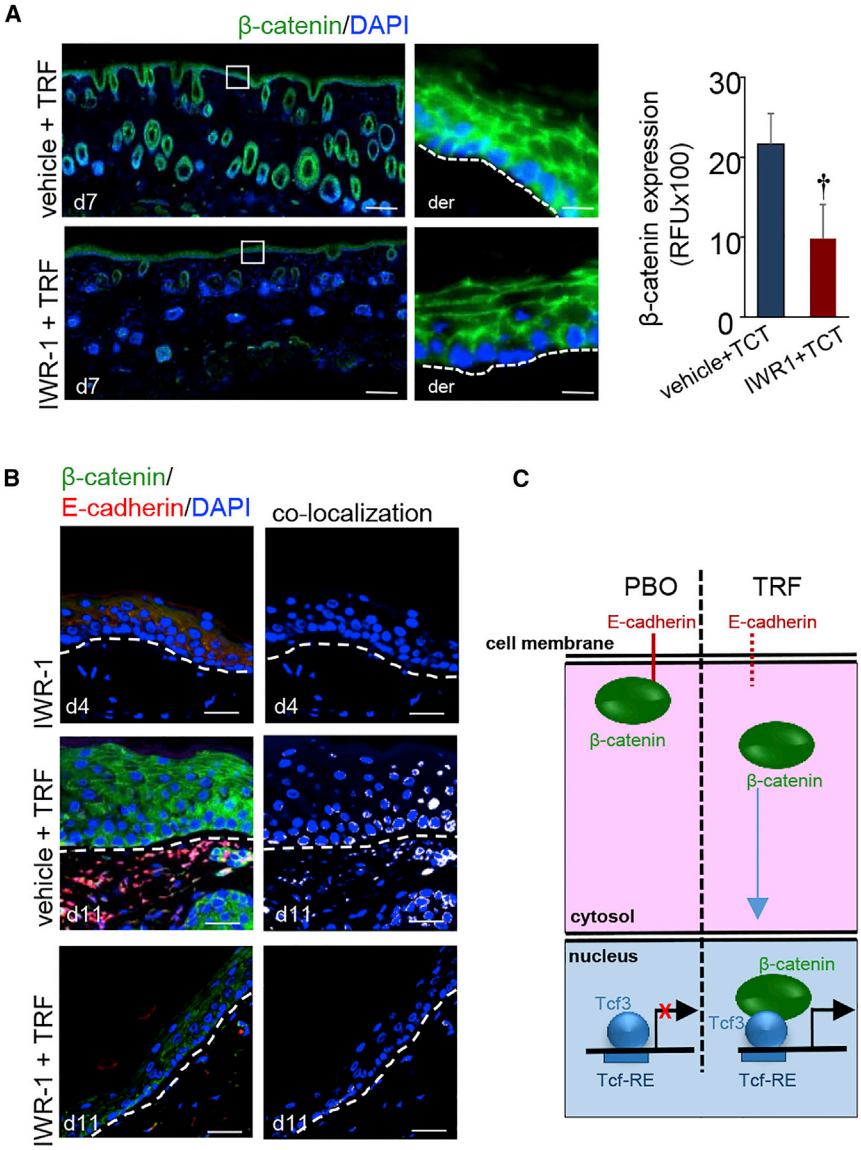

Figure 7. β-Catenin Inhibition Arrested Inducible Anagen Hair Cycling

(A) IWR-1, a β-catenin inhibitor, significantly attenuated TRF-induced epidermal β-catenin (green) expression in the adult skin. Counterstained with DAPI (blue). Scale bars, 500 μm. β-Catenin signal was quantified and plotted graphically. Data are mean ± SD (n = 3; †$p < 0.01$). The dermal (der) and epidermal junctions are marked by a dashed line in the inset pictures. Scale bars, 20 μm. (B) IWR-1 inhibited TRF-induced translocation of β-catenin to the nucleus. Scale bar, 50 μm. (C) Proposed schematic diagram of TRF-induced hair folliculogenesis.

followed by topical TRF or PBO application, as indicated in figure legends.

In Vivo Imaging

Fifteen minutes before imaging, the *rep*TOP*mito*IRE mice were injected intraperitoneally with the potassium salt of beetle luciferin.[53] The animals were imaged under anesthesia using the IVIS Lumina II optical imaging system, and the overlay images were made using Living Image software.

Detection of Anagen Induction

Promotion of hair growth was evaluated by observing the skin color, which is indicative of the telogen-to-anagen conversion.[50] Skin was collected, and 8-μm formalin-fixed paraffin-embedded skin sections were deparaffinized and stained with H&E. Mosaic images at 20× were collected using the Axio Scan.Z1 slide scanner (Zeiss Microscopy). From histological characterization of the sections, anagen follicles in dermis and subcutis layers were enumerated.

Cell and Cell Culture

Immortalized human keratinocytes (HaCaT cells) were grown in low-glucose DMEM (Life Technologies), as described previously.[55] Cells were maintained in a standard culture incubator with humidified air containing 5% CO_2 at 37°C.

Synthesis of Tcf3 Decoy and Control Double-Stranded Oligodeoxynucleotides

Tcf3 decoy and control double-stranded oligodeoxynucleotides were prepared as described previously.[22] Briefly, FAM-labeled phosphorothioate oligodeoxynucleotides were synthesized and purified by Sigma-Aldrich. The oligonucleotide sequences used were the following: Tcf3 decoy sense, 5′- 6FAM-CCGGGCTTTGATCTTTGC-3′; Tcf3 decoy anti-sense, 5′-6FAM-GCAAAGATCAAAGCCCGG-3′; Tcf3 scramble sense, 5′-6FAM-CCGGGTCAGTTCTTTTGC-3′; and Tcf3 scramble anti-sense, 5′-6FAM-GCAAAAGAACTGACCCGG-3′. Double-stranded oligodeoxynucleotides were prepared by dissolving sense and antisense oligodeoxynucleotides in TE buffer (Integrated DNA Technologies) at a concentration of 1 mmol/L. Each sense-antisense pair was annealed by heating at 95°C for 10 min. The reaction mixture was then allowed to cool to room temperature.

Transfection of siRNA and Double-Stranded Oligodeoxynucleotides

DharmaFECT 1 transfection reagent was used to transfect HaCaT cells with ON-TARGETplus siRNA (small interfering RNA) for E-cadherin (Dharmacon), as described previously.[56] Cells were re-seeded onto chamber slides 48 hr after transfection. Next, cells were fixed after 24 hr or 72 hr after transfection. Double-stranded oligodeoxynucleotides were transfected to HaCaT cells using Lipofectamine LTX with Plus Reagent (Invitrogen), as

described previously.[11] Cells were processed for ICC 48 hr after transfection.[11]

Trans-epidermal Water Loss

DermaLab TEWL Probe (cyberDERM) was used to measure the trans-epidermal water loss (TEWL) from the skin, as described previously.[57] TEWL was expressed as ($gm^{-2}hr^{-1}$).

In Situ Proximity Ligation Assay

Proximity ligation assay (PLA) was performed as described previously using the Sigma Duolink In Situ Red Starter Kit Goat/Rabbit (DUO92105) following the manufacturer's instructions, except that the incubation time was prolonged to 90 min.[58] The assay was performed using rabbit Tcf3 (Abcam, ab69999; 1:50) and mouse β-catenin (Abcam, ab22656; 1:200) antibodies. Slides were imaged using an Olympus FV 1000 spectral confocal microscope.

Laser Capture Microdissection of the Epidermis

Laser capture microdissection (LCM) was performed using a laser microdissection system from PALM Technologies, containing a PALM MicroBeam and RoboStage for high-throughput sample collection and a PALM RoboMover (PALM Robo software, v2.2) as described previously.[59] For epidermal LCM, sections were stained with hematoxylin for 30 s, subsequently washed with DEPC-H_2O, and dehydrated in ethanol. The epidermis was identified based on the histology. Epidermal tissue elements were typically cut and captured under a 20× ocular lens. Samples were catapulted into 25 μL of cell direct lysis extraction buffer (Invitrogen). Approximately 100,000 μm^2 of tissue area was captured into each cap, and the extract was then held at −80°C for further analyses.

Real-Time qPCR

For mRNA expression studies, total cDNA synthesis was achieved using the SuperScript Vilo cDNA Synthesis Kit (Invitrogen). The transcript levels of *Oct4*, *Sox9*, and *LGR6* were assessed by real-time PCR using SYBR Green-I (Applied Biosystems). GAPDH served as housekeeping control. The following primer sets were used: m_GAPDH F, 5′-ATGACCACAGTCCATGCCATCACT-3′; m_GAPDH R, 5′- TGTTGAAGTCGCAGGAGACAACCT-3′; m_Oct4 F, 5′-TGGATCCTCGAACCTGGCTA-3′; m_Oct4 R, 5′-CTCAGGCTGCAAAGTCTCCA-3′; m_Sox9 F, 5′-CCCCATCGACTTCCGCGACG-3′; m_Sox9 R, 5′-TGGGTGCGGTGCTGCTGATG-3′; m_LGR6 F, 5′-CGTCGGTGCTGCTGCTCACA-3′; and m_LGR6 R, 5′-CGGCCACCACCAGGAAGCAG-3′.

Immunoprecipitation and Immunoblots

HaCaT cells (0.5×10^6 cells per well) were seeded in six-well plates and treated with either 1 μM tocotrienol (TCT) or an equivalent volume of ethanol for 24 hr. Immunoprecipitation and subsequent immunoblots were performed as described previously.[11] Briefly, the nuclear fractions from the cells were extracted (Signosis Nuclear Extraction Kit, SK001), and 100 μg pooled nuclear extract was incubated with 500 ng β-catenin antibody (Abcam; ab32571) overnight at 4°C and then incubated at 4°C with 30 μL anti-rabbit IgG beads (TrueBlot Ig IP Beads; eBioscience). Immunoprecipitated complexes were washed four times with lysis buffer (centrifugation at 1000 × *g* at 4°C for 5 min), recovered in 25 μL 4× Laemmli buffer with 50 mM fresh DTT, and boiled for 10 min. Next, equal volumes of samples were loaded onto SDS-PAGE gel and immunoblotted.

Histology, Immunohistochemistry, and ICC

Histology of skin was performed from 8-μm-thick paraffin sections after staining with H&E. Immunostainings of Ki67 (Abcam, ab15580; 1:400), LGR6 (Abcam, ab126747; 1:100), CD34 (Abcam, ab8158; 1:200), OCT4 (Abcam, ab19857; 1:200), SOX9 (Abcam, ab185230; 1:1,000), KLF4 (Abcam; ab151733, 1:200), c-MYC (Abcam; ab32072, 1:200), NANOG (Abcam; ab80892, 1:200), K17 (Abcam, ab53707; 1:100), K15 (Abcam, ab52816; 1:100), claudin (Invitrogen, RB9209P; 1:200), occludin (Invitrogen, 711500; 1:200), ZO-1 (Invitrogen, 617300; 1:200), ZO-2 (Invitrogen, 389100; 1:200), E-cadherin (Life Technologies, 131900; 1:200), and β-catenin (Abcam, ab22656; 1:200) were performed on paraffin and cryosections of skin sample using specific antibodies as indicated.[57] For ICC, cells were fixed with cell fixation buffer (eBioscience; 00-8222-49) and stained for respective antibodies. Specificity of the antibodies was validated using rabbit isotype control (Abcam, ab27478; 1:400), rat isotype control (Abcam, ab18412; 1:200), and mouse isotype control (Abcam, ab18443; 1:200) (Figure S6). Briefly, optimal cutting temperature (OCT)-embedded tissues were cryosectioned (10 μm), fixed with cold acetone, blocked with 10% normal goat serum, and incubated with specific antibodies overnight at 4°C. Signal was visualized by subsequent incubation with either biotinylated-tagged (for 3,3′-diaminobenzidine [DAB] staining) or fluorescence-tagged appropriate secondary antibodies (Alexa 488-tagged α-mouse, 1:200; Alexa 568-tagged α-mouse, 1:200; Alexa 488-tagged α-rabbit, 1:200; Alexa 568-tagged α-rabbit, 1:200; Alexa 568-tagged α-rat, 1:200).

Statistical Analyses

Data are expressed as mean ± SD of at least four to six animals per group, as indicated in the figure legends. Significance between two groups was tested using Student's t test (two-tailed). A value of $p < 0.05$ was considered statistically significant. Significant responses ($p < 0.05$) are marked by symbols (†, §, *), and their corresponding p values are provided in the figure legends.

SUPPLEMENTAL INFORMATION

Supplemental Information includes six figures and can be found with this article online at http://dx.doi.org/10.1016/j.ymthe.2017.07.010.

AUTHOR CONTRIBUTIONS

Conceptualization, C.K.S., N.S.A., S.G., and S.K.; Methodology, C.K.S., S.G., N.S.A., M.S.E.M., and S.K.; Investigation and Validation, N.S.A., S.G., M.S.E.M., and S.C.G.; Formal Analysis, S.G., M.S.E.M., S.R., H.E., and S.K.; Writing – Original Draft, N.S.A, S.G., M.S.E.M., S.R., M.A., H.E., C.K.S., and S.K.; Writing – Review & Editing, S.G., M.S.E.M., C.K.S., and S.K.; Visualization, S.G. and S.K.; Funding Acquisition, C.K.S. and S.K.; Resources, C.K.S. and S.K.; Supervision, C.K.S., S.R., and S.K.

CONFLICTS OF INTEREST

The authors declare no conflict of interest.

ACKNOWLEDGMENTS

We thank Hovid Bhd for providing the Tocovid and placebo capsules. Excelvite, Inc., supplied purified tocotrienol for in vitro studies. This study was supported in part by the NIH RO1 grants GM069589, GM077185, NR013898, and NS42617 to C.K.S. and NS085272 to S.K.

REFERENCES

1. Mistriotis, P., and Andreadis, S.T. (2013). Hair follicle: a novel source of multipotent stem cells for tissue engineering and regenerative medicine. Tissue Eng. Part B Rev. *19*, 265–278.
2. Schneider, M.R., Schmidt-Ullrich, R., and Paus, R. (2009). The hair follicle as a dynamic miniorgan. Curr. Biol. *19*, R132–R142.
3. Millar, S.E. (2002). Molecular mechanisms regulating hair follicle development. J. Invest. Dermatol. *118*, 216–225.
4. Fuchs, E. (2008). Skin stem cells: rising to the surface. J. Cell Biol. *180*, 273–284.
5. McGowan, K.M., and Coulombe, P.A. (1998). Onset of keratin 17 expression coincides with the definition of major epithelial lineages during skin development. J. Cell Biol. *143*, 469–486.
6. Snippert, H.J., Haegebarth, A., Kasper, M., Jaks, V., van Es, J.H., Barker, N., van de Wetering, M., van den Born, M., Begthel, H., Vries, R.G., et al. (2010). Lgr6 marks stem cells in the hair follicle that generate all cell lineages of the skin. Science *327*, 1385–1389.
7. Lo Celso, C., Prowse, D.M., and Watt, F.M. (2004). Transient activation of beta-catenin signalling in adult mouse epidermis is sufficient to induce new hair follicles but continuous activation is required to maintain hair follicle tumours. Development *131*, 1787–1799.
8. Silva-Vargas, V., Lo Celso, C., Giangreco, A., Ofstad, T., Prowse, D.M., Braun, K.M., and Watt, F.M. (2005). Beta-catenin and Hedgehog signal strength can specify number and location of hair follicles in adult epidermis without recruitment of bulge stem cells. Dev. Cell *9*, 121–131.
9. Ito, M., Yang, Z., Andl, T., Cui, C., Kim, N., Millar, S.E., and Cotsarelis, G. (2007). Wnt-dependent de novo hair follicle regeneration in adult mouse skin after wounding. Nature *447*, 316–320.
10. Sen, C.K., Khanna, S., and Roy, S. (2006). Tocotrienols: vitamin E beyond tocopherols. Life Sci. *78*, 2088–2098.
11. Khanna, S., Roy, S., Park, H.A., and Sen, C.K. (2007). Regulation of c-Src activity in glutamate-induced neurodegeneration. J. Biol. Chem. *282*, 23482–23490.
12. Khanna, S., Roy, S., Ryu, H., Bahadduri, P., Swaan, P.W., Ratan, R.R., and Sen, C.K. (2003). Molecular basis of vitamin E action: tocotrienol modulates 12-lipoxygenase, a key mediator of glutamate-induced neurodegeneration. J. Biol. Chem. *278*, 43508–43515.
13. Khanna, S., Roy, S., Slivka, A., Craft, T.K., Chaki, S., Rink, C., Notestine, M.A., DeVries, A.C., Parinandi, N.L., and Sen, C.K. (2005). Neuroprotective properties of the natural vitamin E alpha-tocotrienol. Stroke *36*, 2258–2264.
14. Sen, C.K., Khanna, S., and Roy, S. (2004). Tocotrienol: the natural vitamin E to defend the nervous system? Ann. N Y Acad. Sci. *1031*, 127–142.
15. Sen, C.K., Rink, C., and Khanna, S. (2010). Palm oil-derived natural vitamin E α-tocotrienol in brain health and disease. J. Am. Coll. Nutr. *29* (3, Suppl.), 314S–323S.
16. Beoy, L.A., Woei, W.J., and Hay, Y.K. (2010). Effects of tocotrienol supplementation on hair growth in human volunteers. Trop. Life Sci. Res. *21*, 91–99.
17. Tartaglia, L.A., Dembski, M., Weng, X., Deng, N., Culpepper, J., Devos, R., Richards, G.J., Campfield, L.A., Clark, F.T., Deeds, J., et al. (1995). Identification and expression cloning of a leptin receptor, OB-R. Cell *83*, 1263–1271.
18. Li, H.-H., Fu, X.-B., Zhang, L., and Zhou, G. (2008). Comparison of proliferating cells between human adult and fetal eccrine sweat glands. Arch. Dermatol. Res. *300*, 173–176.
19. Tsai, S.-Y., Sennett, R., Rezza, A., Clavel, C., Grisanti, L., Zemla, R., Najam, S., and Rendl, M. (2014). Wnt/β-catenin signaling in dermal condensates is required for hair follicle formation. Dev. Biol. *385*, 179–188.
20. Cole, M.F., Johnstone, S.E., Newman, J.J., Kagey, M.H., and Young, R.A. (2008). Tcf3 is an integral component of the core regulatory circuitry of embryonic stem cells. Genes Dev. *22*, 746–755.
21. Chen, L., and Daley, G.Q. (2008). Molecular basis of pluripotency. Hum. Mol. Genet. *17* (R1), R23–R27.
22. Seki, Y., Yamamoto, H., Ngan, C.Y., Yasui, M., Tomita, N., Kitani, K., Takemasa, I., Ikeda, M., Sekimoto, M., Matsuura, N., et al. (2006). Construction of a novel DNA decoy that inhibits the oncogenic beta-catenin/T-cell factor pathway. Mol. Cancer Ther. *5*, 985–994.
23. Cadigan, K.M., and Waterman, M.L. (2012). TCF/LEFs and Wnt signaling in the nucleus. Cold Spring Harb. Perspect. Biol. *4*, a007906.
24. Krause, K., and Foitzik, K. (2006). Biology of the hair follicle: the basics. Semin. Cutan. Med. Surg. *25*, 2–10.
25. Stenn, K.S., and Paus, R. (2001). Controls of hair follicle cycling. Physiol. Rev. *81*, 449–494.
26. Paus, R., and Foitzik, K. (2004). In search of the "hair cycle clock": a guided tour. Differentiation *72*, 489–511.
27. Liu, S., Zhang, H., and Duan, E. (2013). Epidermal development in mammals: key regulators, signals from beneath, and stem cells. Int. J. Mol. Sci. *14*, 10869–10895.
28. Collins, C.A., Kretzschmar, K., and Watt, F.M. (2011). Reprogramming adult dermis to a neonatal state through epidermal activation of β-catenin. Development *138*, 5189–5199.
29. Van Mater, D., Kolligs, F.T., Dlugosz, A.A., and Fearon, E.R. (2003). Transient activation of beta -catenin signaling in cutaneous keratinocytes is sufficient to trigger the active growth phase of the hair cycle in mice. Genes Dev. *17*, 1219–1224.
30. Orsulic, S., Huber, O., Aberle, H., Arnold, S., and Kemler, R. (1999). E-cadherin binding prevents beta-catenin nuclear localization and beta-catenin/LEF-1-mediated transactivation. J. Cell Sci. *112*, 1237–1245.
31. Wu, C.-I., Hoffman, J.A., Shy, B.R., Ford, E.M., Fuchs, E., Nguyen, H., and Merrill, B.J. (2012). Function of Wnt/β-catenin in counteracting Tcf3 repression through the Tcf3-β-catenin interaction. Development *139*, 2118–2129.
32. Brannon, M., Gomperts, M., Sumoy, L., Moon, R.T., and Kimelman, D. (1997). A beta-catenin/XTcf-3 complex binds to the *siamois* promoter to regulate dorsal axis specification in *Xenopus*. Genes Dev. *11*, 2359–2370.
33. Molenaar, M., van de Wetering, M., Oosterwegel, M., Peterson-Maduro, J., Godsave, S., Korinek, V., Roose, J., Destrée, O., and Clevers, H. (1996). XTcf-3 transcription factor mediates beta-catenin-induced axis formation in Xenopus embryos. Cell *86*, 391–399.
34. Tian, X., Liu, Z., Niu, B., Zhang, J., Tan, T.K., Lee, S.R., Zhao, Y., Harris, D.C., and Zheng, G. (2011). E-cadherin/β-catenin complex and the epithelial barrier. J. Biomed. Biotechnol. *2011*, 567305.
35. Strauss, R., Hamerlik, P., Lieber, A., and Bartek, J. (2012). Regulation of stem cell plasticity: mechanisms and relevance to tissue biology and cancer. Mol. Ther. *20*, 887–897.
36. Chen, B., Dodge, M.E., Tang, W., Lu, J., Ma, Z., Fan, C.-W., Wei, S., Hao, W., Kilgore, J., Williams, N.S., et al. (2009). Small molecule-mediated disruption of Wnt-dependent signaling in tissue regeneration and cancer. Nat. Chem. Biol. *5*, 100–107.
37. Jamora, C., DasGupta, R., Kocieniewski, P., and Fuchs, E. (2003). Links between signal transduction, transcription and adhesion in epithelial bud development. Nature *422*, 317–322.
38. Rivera-Gonzalez, G., Shook, B., and Horsley, V. (2014). Adipocytes in skin health and disease. Cold Spring Harb. Perspect. Med. *4*, a015271.
39. Sumikawa, Y., Inui, S., Nakajima, T., and Itami, S. (2014). Hair cycle control by leptin as a new anagen inducer. Exp. Dermatol. *23*, 27–32.
40. Driskell, R.R., Clavel, C., Rendl, M., and Watt, F.M. (2011). Hair follicle dermal papilla cells at a glance. J. Cell Sci. *124*, 1179–1182.

41. Huelsken, J., Vogel, R., Erdmann, B., Cotsarelis, G., and Birchmeier, W. (2001). β-Catenin controls hair follicle morphogenesis and stem cell differentiation in the skin. Cell *105*, 533–545.

42. Alonso, L., and Fuchs, E. (2006). The hair cycle. J. Cell Sci. *119*, 391–393.

43. Blanpain, C., and Fuchs, E. (2006). Epidermal stem cells of the skin. Annu. Rev. Cell Dev. Biol. *22*, 339–373.

44. Oshima, H., Rochat, A., Kedzia, C., Kobayashi, K., and Barrandon, Y. (2001). Morphogenesis and renewal of hair follicles from adult multipotent stem cells. Cell *104*, 233–245.

45. Taylor, G., Lehrer, M.S., Jensen, P.J., Sun, T.T., and Lavker, R.M. (2000). Involvement of follicular stem cells in forming not only the follicle but also the epidermis. Cell *102*, 451–461.

46. Lay, K., Kume, T., and Fuchs, E. (2016). FOXC1 maintains the hair follicle stem cell niche and governs stem cell quiescence to preserve long-term tissue-regenerating potential. Proc. Natl. Acad. Sci. USA *113*, E1506–E1515.

47. Geyfman, M., Plikus, M.V., Treffeisen, E., Andersen, B., and Paus, R. (2015). Resting no more: re-defining telogen, the maintenance stage of the hair growth cycle. Biol. Rev. Camb. Philos. Soc. *90*, 1179–1196.

48. Paus, R., and Cotsarelis, G. (1999). The biology of hair follicles. N. Engl. J. Med. *341*, 491–497.

49. Porter, R.M. (2003). Mouse models for human hair loss disorders. J. Anat. *202*, 125–131.

50. Müller-Röver, S., Handjiski, B., van der Veen, C., Eichmüller, S., Foitzik, K., McKay, I.A., Stenn, K.S., and Paus, R. (2001). A comprehensive guide for the accurate classification of murine hair follicles in distinct hair cycle stages. J. Invest. Dermatol. *117*, 3–15.

51. Garza, L.A., Liu, Y., Yang, Z., Alagesan, B., Lawson, J.A., Norberg, S.M., Loy, D.E., Zhao, T., Blatt, H.B., Stanton, D.C., et al. (2012). Prostaglandin D2 inhibits hair growth and is elevated in bald scalp of men with androgenetic alopecia. Sci. Transl. Med. *4*, 126ra34.

52. Halloy, J., Bernard, B.A., Loussouarn, G., and Goldbeter, A. (2000). Modeling the dynamics of human hair cycles by a follicular automaton. Proc. Natl. Acad. Sci. USA *97*, 8328–8333.

53. Ghatak, S., Li, J., Chan, Y.C., Gnyawali, S.C., Steen, E., Yung, B.C., Khanna, S., Roy, S., Lee, R.J., and Sen, C.K. (2016). AntihypoxamiR functionalized gramicidin lipid nanoparticles rescue against ischemic memory improving cutaneous wound healing. Nanomedicine (Lond.) *12*, 1827–1831.

54. Patel, V., Rink, C., Gordillo, G.M., Khanna, S., Gnyawali, U., Roy, S., Shneker, B., Ganesh, K., Phillips, G., More, J.L., et al. (2012). Oral tocotrienols are transported to human tissues and delay the progression of the model for end-stage liver disease score in patients. J. Nutr. *142*, 513–519.

55. Sen, C.K., Khanna, S., Babior, B.M., Hunt, T.K., Ellison, E.C., and Roy, S. (2002). Oxidant-induced vascular endothelial growth factor expression in human keratinocytes and cutaneous wound healing. J. Biol. Chem. *277*, 33284–33290.

56. Chan, Y.C., Khanna, S., Roy, S., and Sen, C.K. (2011). miR-200b targets Ets-1 and is down-regulated by hypoxia to induce angiogenic response of endothelial cells. J. Biol. Chem. *286*, 2047–2056.

57. Ghatak, S., Chan, Y.C., Khanna, S., Banerjee, J., Weist, J., Roy, S., and Sen, C.K. (2015). Barrier function of the repaired skin is disrupted following arrest of Dicer in keratinocytes. Mol. Ther. *23*, 1201–1210.

58. Gordillo, G.M., Biswas, A., Khanna, S., Spieldenner, J.M., Pan, X., and Sen, C.K. (2016). Multidrug resistance-associated protein-1 (MRP-1)-dependent glutathione disulfide (GSSG) efflux as a critical survival factor for oxidant-enriched tumorigenic endothelial cells. J. Biol. Chem. *291*, 10089–10103.

59. Kuhn, D.E., Roy, S., Radtke, J., Khanna, S., and Sen, C.K. (2007). Laser microdissection and capture of pure cardiomyocytes and fibroblasts from infarcted heart regions: perceived hyperoxia induces p21 in peri-infarct myocytes. Am. J. Physiol. Heart Circ. Physiol. *292*, H1245–H1253.

YMTHE, Volume *25*

Supplemental Information

Epidermal E-Cadherin Dependent β-Catenin Pathway Is Phytochemical Inducible and Accelerates Anagen Hair Cycling

Noha S. Ahmed, Subhadip Ghatak, Mohamed S. El Masry, Surya C. Gnyawali, Sashwati Roy, Mohamed Amer, Helen Everts, Chandan K. Sen, and Savita Khanna

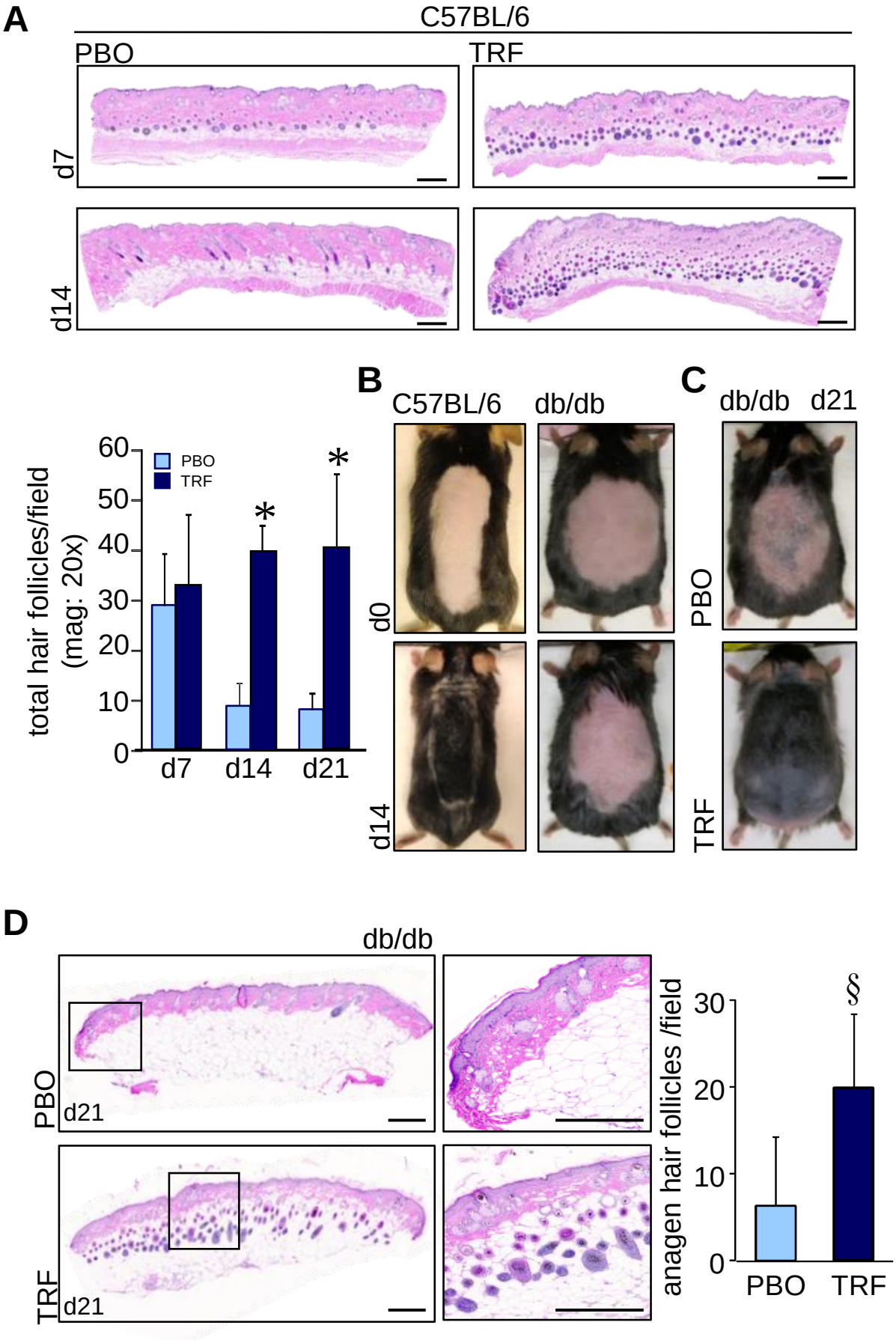

Supplemental Figure 1

Figure S1: (**A**) Representative photomicrograph of formalin fixed paraffin embedded H&E stained sections showing larger number of anagen hair follicle in TRF treated (days 7 and 14) sections. Scale bar = 500μm. Total number of hair follicles were quantified from the H&E stained sections from each week and plotted graphically. Data are mean ± SD. (n=6) * $p < 0.001$. (**B**) Digital photomicrographs of C57BL/6 (wt) and db/db mice. db/db mice showing less hair growth in naired skin on day 14. (**C**) Application of TRF induced (day 21) hair growth in dorsal skin of diabetic mouse. (**D**) Representative photomicrograph of formalin fixed paraffin embedded H&E stained sections showing large number of anagen hair follicle in TRF-treated (day 21) db/db skin. Scale bar = 500μm. The number of anagen hair follicles on day 21 were quantified from H&E stained sections and plotted graphically. Data are mean ± SD. (n=6) § $p < 0.05$.

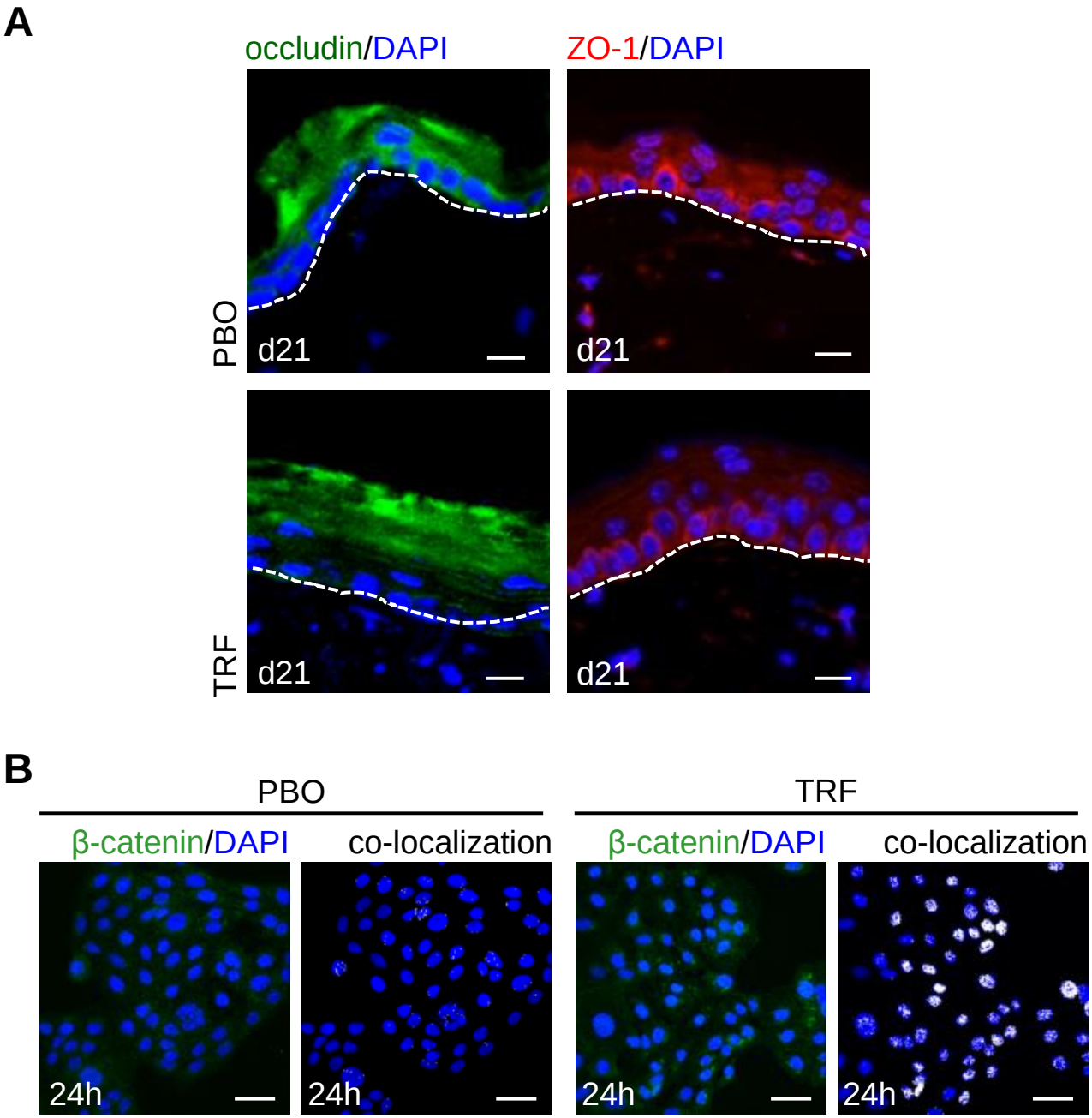

Supplemental Figure 2

Figure S2: (**A**) Representative photograph of formalin fixed paraffin embedded adult skin sections showing no change (day 21) in occludin and ZO-1 expression in the epidermis treated with TRF. Counterstained with DAPI. The dermal and epidermal junction is indicated by a dashed line. Scale bar = 20μm. (**B**) HaCaT keratinocytes treated with TRF (equivalent to 1μM tocotrienol) showed increased nuclear translocation of β-catenin (green) compared to PBO at 24h. Co-localization is shown in white. Scale = 50μm.

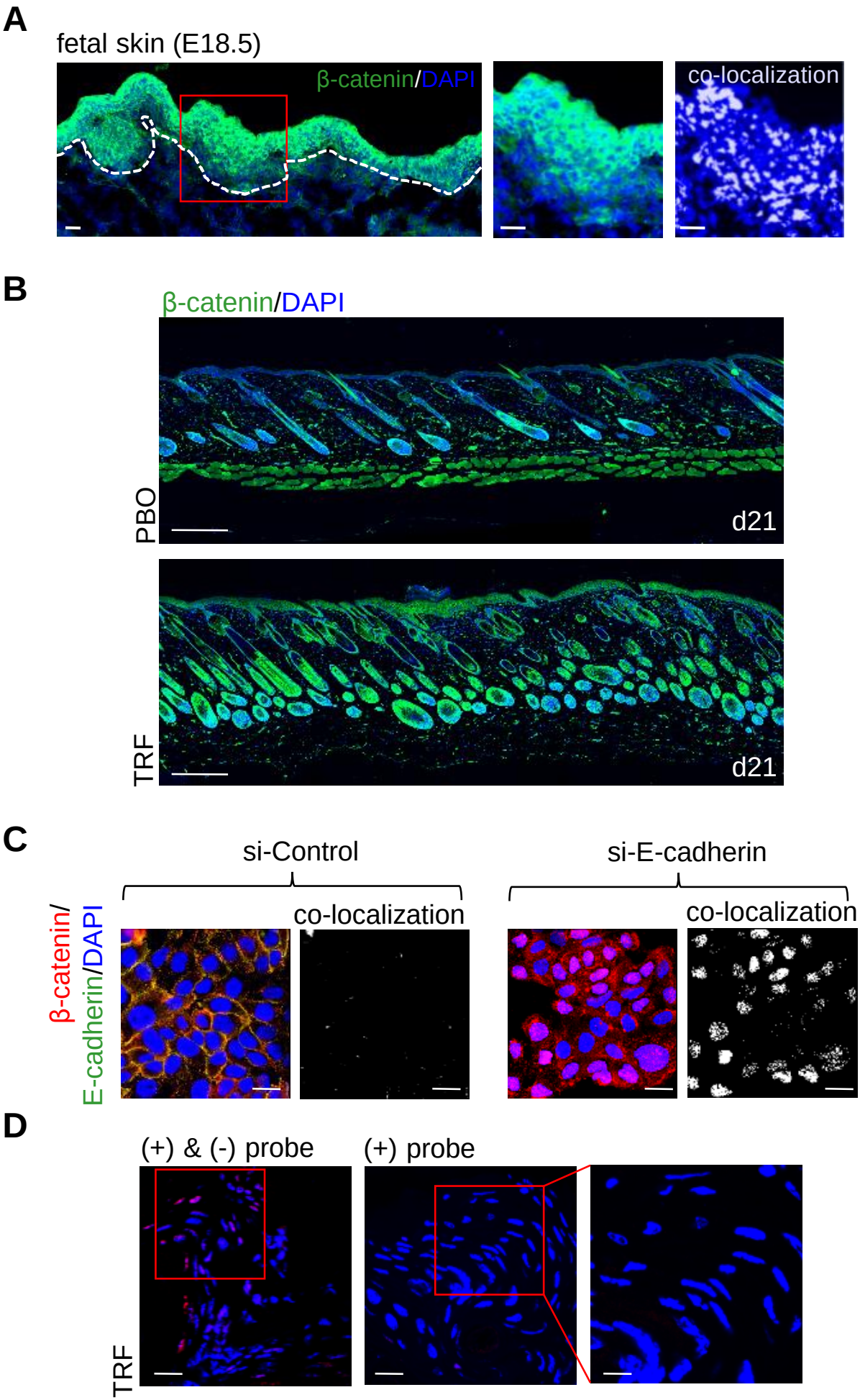
A
fetal skin (E18.5)
β-catenin/DAPI
co-localization
B
β-catenin/DAPI
PBO
d21
TRF
d21
C
si-Control
si-E-cadherin
co-localization
co-localization
β-catenin/
E-cadherin/DAPI
D
(+) & (-) probe
(+) probe
TRF

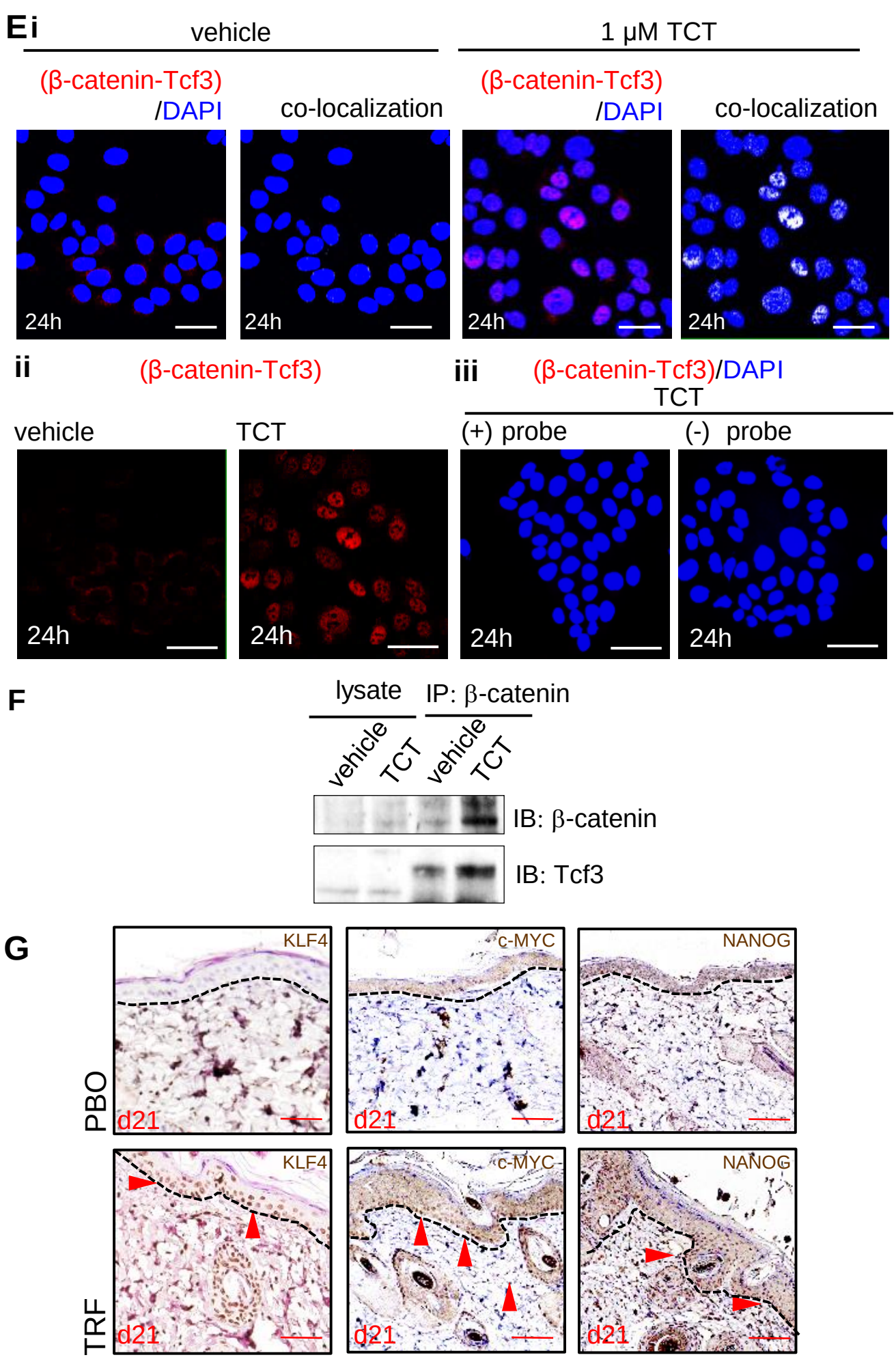
Ei
vehicle
1 μM TCT
(β-catenin-Tcf3)
/DAPI
co-localization
(β-catenin-Tcf3)
/DAPI
co-localization
24h
24h
24h
24h
ii
(β-catenin-Tcf3)
iii
(β-catenin-Tcf3)/DAPI
TCT
vehicle
TCT
(+) probe
(-) probe
24h
24h
24h
24h
F
lysate
IP: β-catenin
vehicle
TCT
vehicle
TCT
IB: β-catenin
IB: Tcf3
G
KLF4
c-MYC
NANOG
PBO
TRF
d21
d21
d21
d21
d21
d21

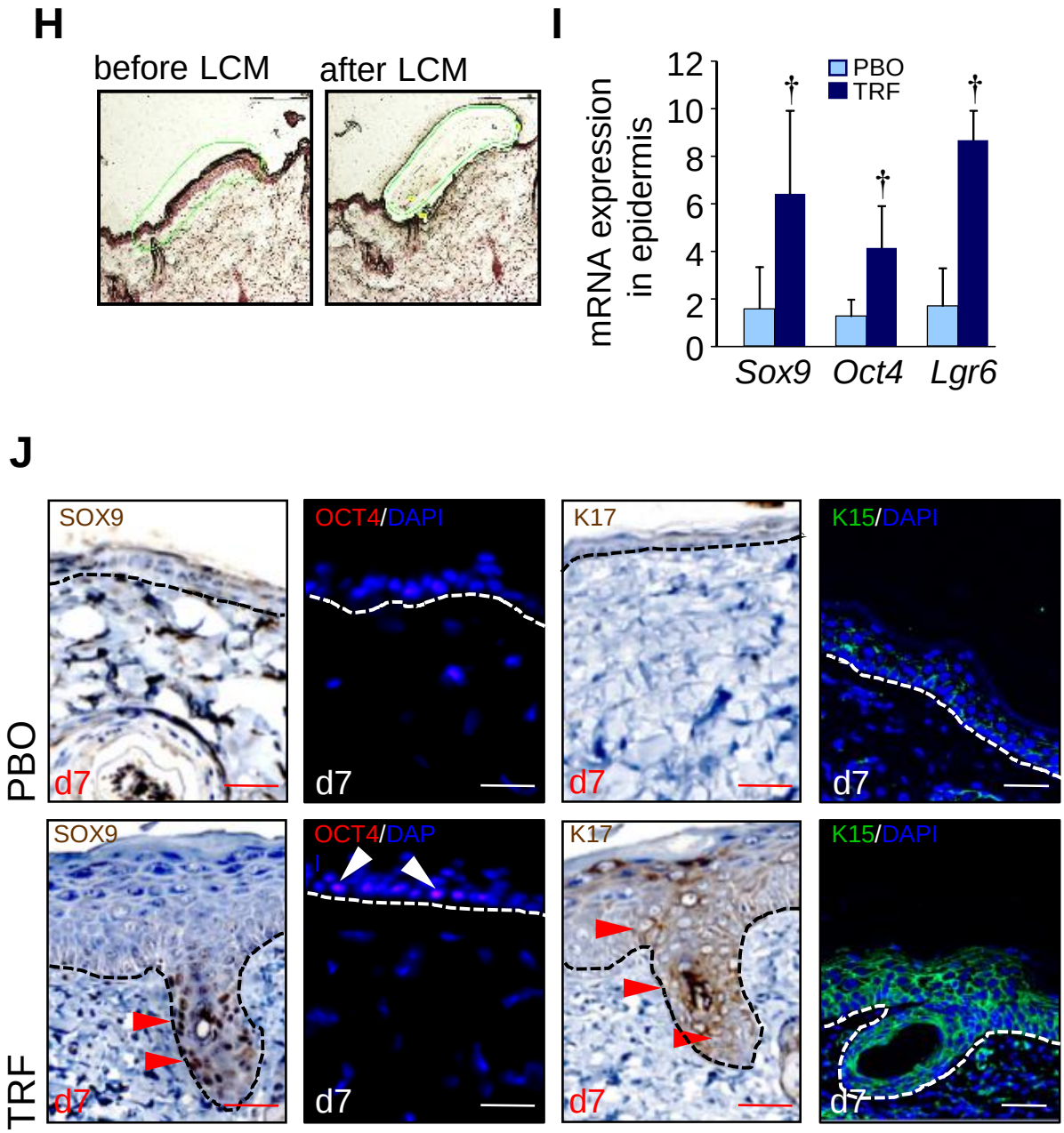
H
before LCM
after LCM
I
mRNA expression in epidermis
12
10
8
6
4
2
0
PBO
TRF
Sox9
Oct4
Lgr6
J
PBO
TRF
SOX9
OCT4/DAPI
K17
K15/DAPI
d7

Figure S3: (**A**) β-catenin is abundantly expressed in fetal skin (E18.5). Confocal microscopic image showing translocation of β-catenin (green) into the nucleus. Counterstained with DAPI. Dermal and epidermal junction is indicated by dashed line in the left panel. Scale bar = 200μm. Co-localization is shown in white in the right panel. Scale bar = 20μm. (**B**) β-catenin expression in the adult skin epidermis counterstained with DAPI at day 21 post-treatment with TRF or PBO. Scale bar = 200μm. (**C**) E-cadherin knockdown in HaCaT keratinocytes induced nuclear translocation of β-catenin. White dots marks co-localization. Scale bar=20μm. (**D**) Proximity ligation assay (PLA) with both + and – probe and + probe alone validating the assay for which data is shown in **Fig. 5C**. (**E**) (*i*) Proximity ligation assay (PLA) showing the interaction of β-catenin and Tcf3 in the nucleus 24h after treatment with 1μM pure tocotrienol. (ii) PLA showing the β-catenin and Tcf3 co-localization as red dots (related to fig S3Ei. (iii) PLA with (+) probe and (–) probe alone validating the assay. Scale bar = 50μm (**F**) The nuclear lysates from HaCaT keratinocytes after 24h treatment with either vehicle or 1μM pure tocotrienol were subjected to immunoprecipitation with β-catenin antibody. The immunoprecipitates (*IP*) were subjected to SDS-PAGE and subjected to immunoblotting (*IB*) for the detection of Tcf3.

(**G**)KLF4, c-MYC, and NANOG expression in adult skin epidermis on day 21 post-treatment with PBO and TRF. Dermal and epidermal junction is indicated by black dashed line. Scale bar = 20μm. (**H**) Laser captured epidermis was subjected to (**I**) quantitative PCR analysis of *Sox9* , *Oct4* and *Lgr6* (day 21 after PBO and TRF treatment). Data are mean ± SD, † $p<0.01$ compared to PBO. (**J**) SOX9, OCT4, K15 and K17 expression in adult skin epidermis on day 7 post-treatment with TRF. Dermal and epidermal junction is indicated by a dashed line. Scale bar = 20μm.

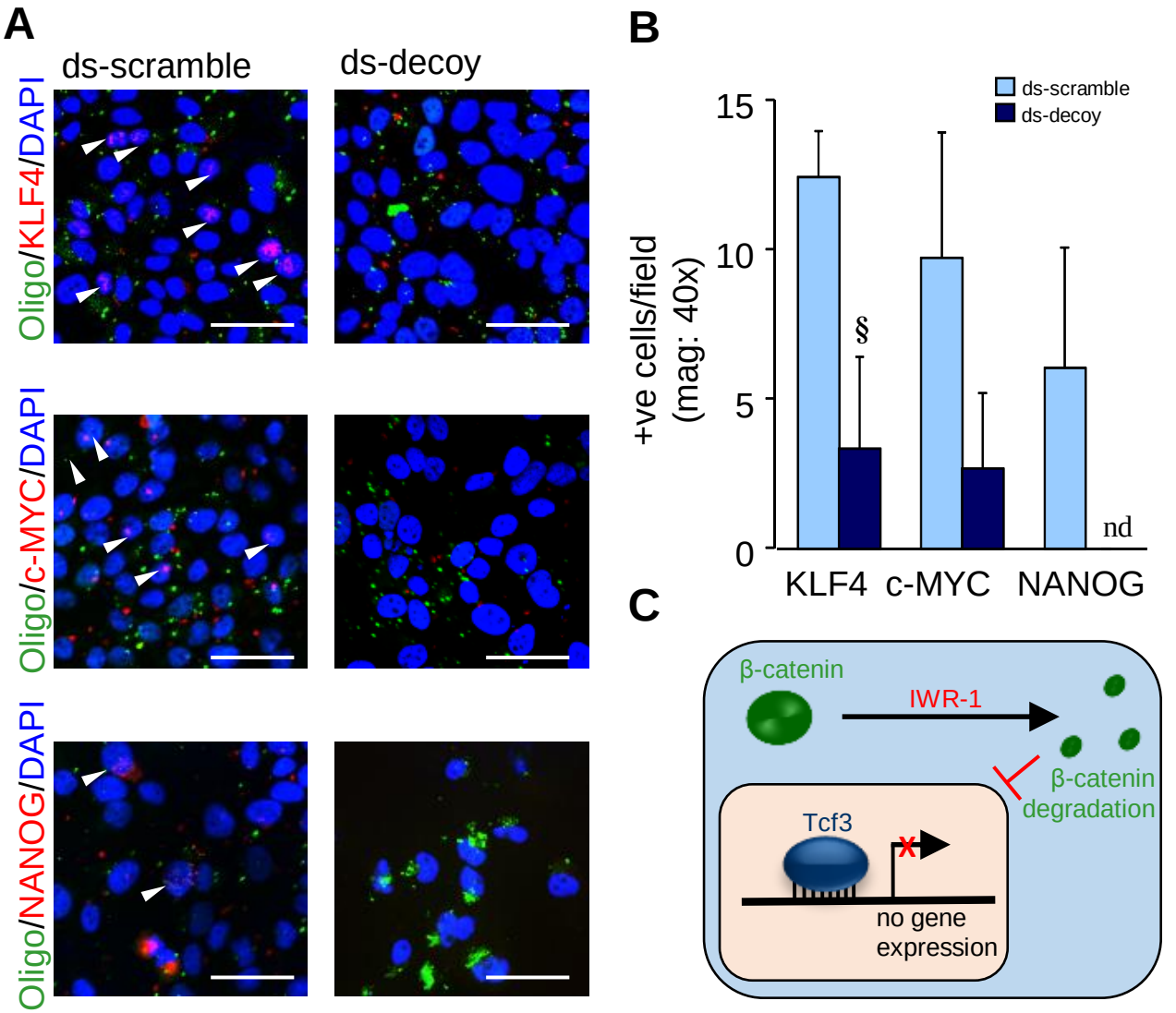

Figure S4: (**A**) Expression of KLF4, c-MYC, and NANOG in Tcf3 scramble and decoy transfected cells after pure tocotrienol treatment (1μM, 24h). Scale bar = 50μm. (**B**) The number of positive cells per field were quantified and plotted graphically. Data are mean ± SD. (n=3) § $p<0.05$. nd, not detected. (**C**) Schematic representation of how IWR-1 is inhibiting β-catenin nuclear translocation and subsequent activation of target gene.

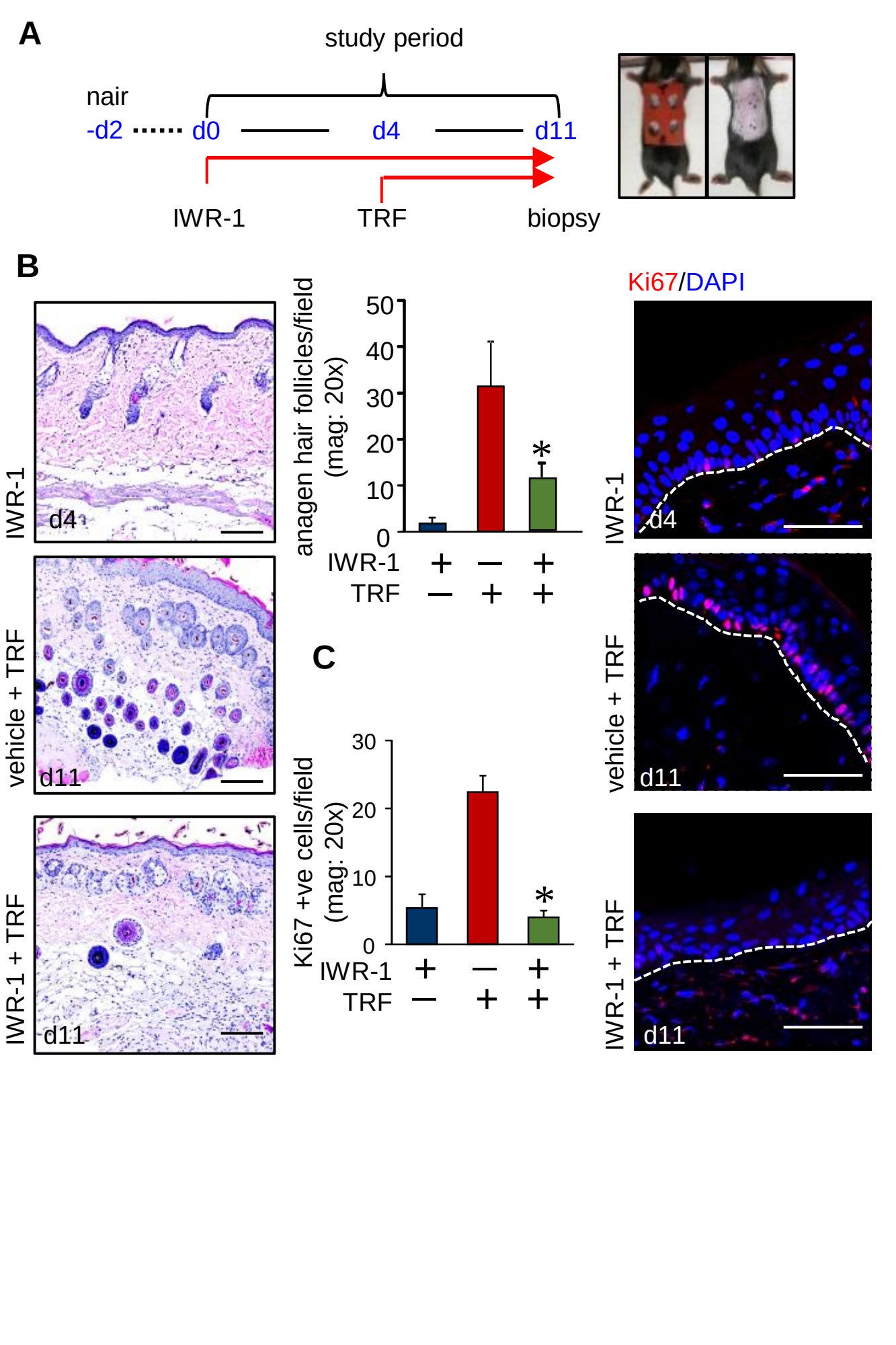
A
study period
nair
-d2
d0
d4
d11
IWR-1
TRF
biopsy
B
IWR-1
d4
vehicle + TRF
d11
IWR-1 + TRF
d11
anagen hair follicles/field
(mag: 20x)
50
40
30
20
10
0
*
IWR-1 + —
TRF — +
Ki67/DAPI
IWR-1
d4
vehicle + TRF
d11
IWR-1 + TRF
d11
C
Ki67 +ve cells/field
(mag: 20x)
30
20
10
0
*
IWR-1 + —
TRF — +

Figure S5: (**A**) Design of topical IWR-1 studies. (**B**) H&E stained skin sections showing that IWR-1 attenuated TRF-induced increase in the number of hair follicles at day 11 (day 7 post TRF application). Scale bar = 50μm. Hair follicles were enumerated and expressed graphically as mean ± SD, * $p<0.001$ compared to vehicle TRF with vehicle. (**C**) Graphical representation of $Ki67^{+}$ (red) cells in formalin fixed paraffin embedded skin sections of mice treated with IWR-1 or vehicle DMSO followed by TRF treatment. IWR-1 treatment blunted TRF-induced cell proliferation in the epidermis. Scale bar = 50μm

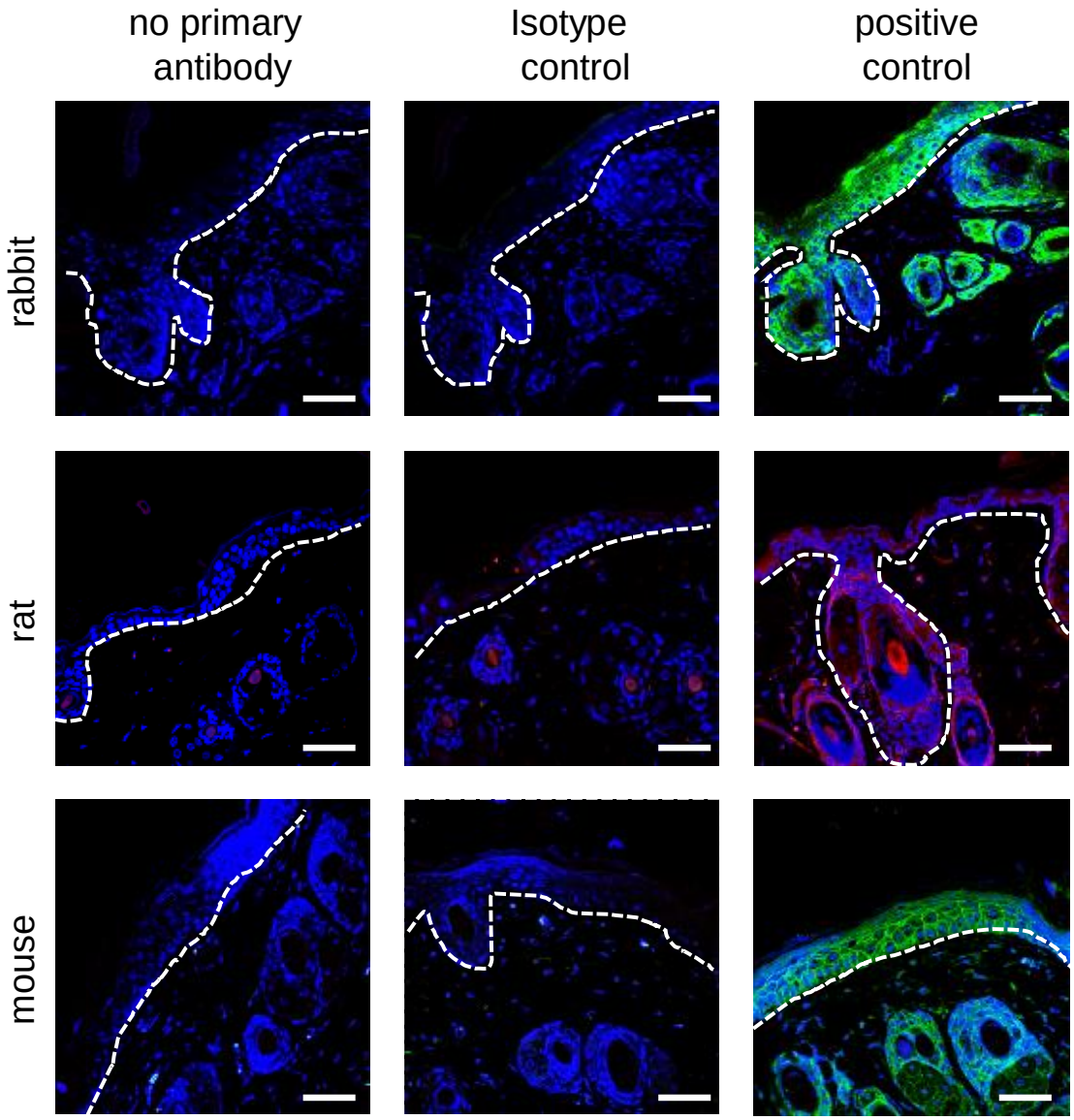

Figure S6: Specificity of the antibodies used in the study was validated using no antibody control and isotype controls of respective host species. The white dash line indicates the epidermal and dermal junctions. Scale bar = 50μm.